Geosynthetic-reinforced embankments over soft foundations

R. K. Rowe[1] and A. L. Li[2]

[1]*GeoEngineering Centre at Queen's-RMC, Department of Civil Engineering, Queen's University, Kingston, Ontario, Canada K7K 3N6, Telephone: + 1 613 533 6933, Telefax: + 1 613 533 6934, E-mail: kerry@civil.queensu.ca (Corresponding author)*
[2]*Project Manager, AMEC Earth & Environmental Limited, Scarborough, Ontario, Canada M1R 3C3, Telephone: + 1 416 751 6565, Telefax: + 1 416 751 7592, E-mail: allen.li@amec.com.*

Received 27 March 2004, accepted 27 March 2004

ABSTRACT: The behaviour of reinforced embankments over conventional soft cohesive soil, rate-sensitive soil and peat deposits is reviewed, and recent design and analysis methods are summarized. The findings from both field observations and finite element analyses are presented. Both undrained and partially drained behaviour of reinforced embankments are considered. The use of reinforcement in combination with prefabricated vertical drains is addressed. The effects of both the viscous and inviscous characteristics of reinforcement and foundation soils on embankment behaviour are discussed. It is concluded that the partial consolidation provided by PVDs and the tension mobilized in reinforcement can substantially increase embankment stability. However, creep of geosynthetics can decrease the embankment failure height. The mobilization of reinforcement during and after embankment construction can vary significantly depending on the soil and reinforcement characteristics. Care must be taken in design when a creep-susceptible reinforcement is being used and/or the foundation soil is rate sensitive. Note: This paper is a slightly modified version of the *Giroud Lecture* presented by R. K. Rowe at the Seventh International Conference on Geosynthetics in Nice, France, in 2002.

KEYWORDS: Geosynthetics, Embankment, Reinforcement, Vertical drains, Soft clay, Stability, Deformations, Plasticity, Creep, Finite element analysis

REFERENCE: Rowe, R.K. and Li, L.L. (2005). Geosynthetic-reinforced embankments over soft foundations. *Geosynthetics International*, Special Issue on the Giroud Lectures, **12**, No. 1, 50–85.

1. INTRODUCTION

The behaviour and design of geosynthetic-reinforced embankments over soft soil have attracted considerable attention in both practice and the literature. The behaviour of basal reinforced embankments over typical soft soils is now well understood: a number of papers have addressed these issues (e.g. Humphrey and Holtz 1987; Jewell 1988; Rowe 1997; Leroueil and Rowe 2001; Rowe and Li 2001), and books such as Jewell (1996) have summarized some common design methodologies. However, it has also been found that these design methods may be overly conservative for conventional soils, and may be unconservative for less conventional soils. The objectives of this paper are six-fold: first, to summarize typical methods of analysis and design for reinforced embankments; second, to discuss the performance of reinforced embankments as observed in field cases; third, to discuss the issues surrounding the selection of 'compatible strain' as a criterion for the design of reinforced embankments; fourth, to examine the effect of partial drainage and the use of prefabricated vertical drains (PVDs) on the design and performance of reinforced embankments on soft clay, and to present a new design methodology; fifth, to summarize design considerations and methods for embankments on fibrous peat; and, finally, to provide new insights regarding the performance and design of reinforced embankments on rate-sensitive soils, and to examine the potential effect of creep in the reinforcement itself.

2. METHODS OF ANALYSIS

2.1. Background

Jewell (1988) described the mechanisms by which reinforcement could improve the performance of embankments on soft soil. This involved the recognition that the lateral earth pressure within an embankment over a soft cohesive foundation imposes shear stresses on the foundation soil, which reduces the bearing capacity of the foundation and hence embankment stability. The basal reinforcement can serve to resist some or all of the earth pressure within the

embankment and to resist the lateral deformations of the foundation, thereby increasing bearing capacity and stability. A number of idealized failure mechanisms can be identified for reinforced embankments: lateral sliding of embankments over the base reinforcement layer, foundation extrusion (bearing capacity failure), rotational slope failure involving breakage or pullout of reinforcement, and excessive displacement.

If the interface shear strength between the reinforcement (e.g. geosynthetic) and fill is inadequate, active earth pressure within the embankment may cause the embankment to slide laterally on top of the reinforcement, although, in practice, this is rarely a critical case. Alternatively, with shallow deposits of low-strength soil, the foundation material can be laterally extruded from beneath the reinforced embankment. If the reinforcement is placed directly on the foundation material then this mechanism may involve horizontal movement of the foundation soil relative to the reinforcement and the overlying embankment. The key parameters controlling these two mechanisms are the shear strength of the foundation soil and the reinforcement–soil interface strength in direct shear.

The factor of safety against a rotational slip failure may be increased by the inclusion of geosynthetic reinforcement. The tensile force required to maintain stability must be developed in the reinforcement by means of shear stresses between the reinforcement and the soil above and below it. Once the interface shear strength is reached, the reinforcement will pull out of the soil and rotational failure will occur. Alternatively, if the tensile strength of the reinforcement is reached, the breakage of the reinforcement will result in a rotational failure. These two possibilities are fairly obvious. There is, however, a third and somewhat less obvious potential failure mechanism. The embankment may fail at a reinforcing force lower than expected based on stability considerations owing to the stress–strain–time characteristics of the reinforcement. If the reinforcement has a low mobilized tensile stiffness, *J*, then large deformations of the foundation may occur prior to reinforcement failure. Under these circumstances, it may not be possible to construct the embankment to the desired height even though 'collapse' has not occurred. Furthermore, for some soils, significant movement along the potential failure surface may result in strain-softening of the soil. Additional load will then be transferred to the reinforcement, leading to even larger strains until eventually the reinforcement will break, accompanied by failure of the embankment. In order to prevent this failure mechanism, consideration must be given to:

(1) the reinforcement–soil interface shear strength under conditions where the reinforcement is pulled out from between the soil above and below it;
(2) the tensile strength of the reinforcement; and
(3) the stress–strain characteristics of the reinforcement relative to those of the foundation soil.

Embankments on highly compressible foundations may fail owing to excessive displacements. For a particular geometry and soil profile, there is a threshold reinforcement tensile stiffness below which the reinforcement has no effect upon settlement. For reinforcement with moduli in excess of this threshold value, the reinforcement will reduce lateral spreading and local yield. This effect will be greatest for shallow deposits or for deposits where the soil strength and stiffness increase with depth. However, the reinforcement cannot eliminate settlement, and there is also an upper threshold tensile stiffness above which any further increase in reinforcement stiffness does not alter the settlement. Thus, under some circumstances, excessive deformations may occur even if high tensile stiffness reinforcement is used. This possibility must be recognized at the design stage, and, if necessary, consideration should be given to the use of a lightweight fill material (e.g. Rowe and Soderman 1985b, 1986).

Many embankments are constructed on deposits which consist of a relatively stiff crust or root mat overlying a weaker and more compressible main deposit. This crust/root mat is a natural reinforcement and will contribute significantly to embankment stability while reducing settlements. However, in doing so, tensions may develop within the crust/root mat. If the limited tensile strength of the crust is exceeded, then tensile failure will occur, followed by the embankment sinking into the soft underlying soil. In these cases, the major role of the reinforcement is to limit the tension developed within the root mat, and this can only be achieved provided the reinforcement is relatively stiff compared with the root mat/crust and provided the tensile strength of the geosynthetic is not reached.

Thus, in addition to the shear strength of the foundation soils, the important properties for the design of reinforced embankments are the soil–reinforcement interface shear strength under direct shear and pullout conditions, the stress–strain characteristics of the reinforcement, and the tensile strength of the reinforcement. The objective of this section is to review existing methods of analyzing the behaviour of reinforced embankments over soft clayey soil.

2.2. Bearing capacity

The first step in the design of an embankment over soft soil is to evaluate whether or not reinforcement or other soil improvement (e.g. PVDs) is required to achieve the design embankment height with the desired factor of safety against collapse under undrained conditions. If the desired factor of safety can be achieved without reinforcement or other soil improvement technique then the analysis stops. If the desired height cannot be safely achieved with an unreinforced design, then one should check whether it is possible to attain the desired height using reinforcement. This can be done by means of a bearing capacity calculation; however, as discussed by Humphrey and Holtz (1987), traditional bearing capacity theory assumes a constant strength with depth and can lead to overconservative estimates of collapse load where the soft foundation has a strength profile that increases with depth and/or is of limited depth.

Plasticity solutions published by Davis and Booker (1973) consider the effect of strength increase with depth

on the bearing capacity of rigid footings. To allow convenient design of reinforced embankments, Rowe and Soderman (1987a) synthesized the bearing capacity factors of Davis and Booker (1973) and Matar and Salencon (1977) for rough footings (Figure 1) and proposed a simple method for estimating the stability of a highly reinforced embankment. This approach, which will be briefly outlined here, considers the effect of increasing undrained shear strength with depth as well as the effect of the relative thickness of the underlying cohesive soil deposit. A reinforced embankment can never be reinforced beyond the point of being rigid: hence these solutions place an upper limit on the improvement in stability which can be achieved using high-strength/tensile stiffness reinforcement.

Since an embankment will generally be trapezoidal in shape and the plasticity solutions are for a rigid footing of width b, an approximation must be made to obtain the equivalent width of the embankment. From plasticity considerations, the pressure at the edge of a rigid footing is $(2 + \pi)s_{uo}$, where s_{uo} is the undrained shear strength directly beneath the footing. It is assumed here that the effective width of the footing, b, will extend between the points on either side of the embankment when the applied pressure γh^* is equal to $(2 + \pi)s_{uo}$. Thus

$$h^* = \frac{(2+\pi)s_{uo}}{\gamma} \tag{1}$$

and hence (from Figure 2)

$$b = B + 2n(H - h^*) \tag{2}$$

where B is the crest width, H is the embankment height, and n is the cotangent of the slope angle (see Figure 2).

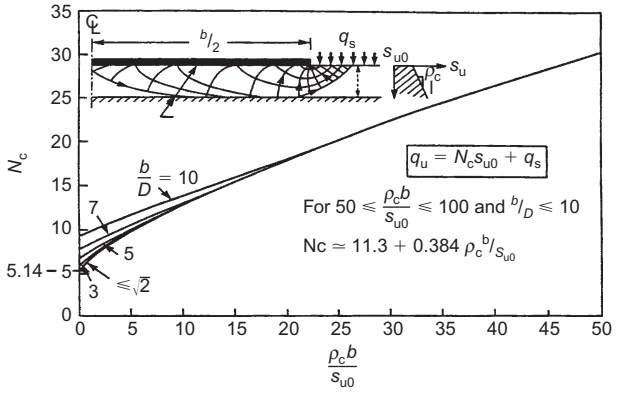

Figure 1. Bearing capacity factor for nonhomogeneous soil (modified from Rowe and Soderman 1987a)

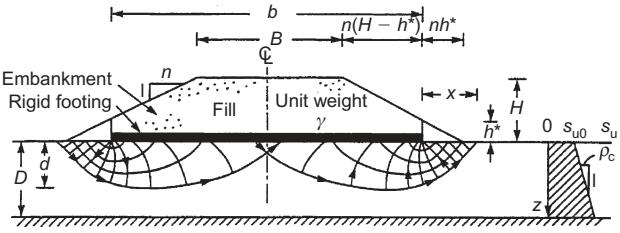

Figure 2. Definition of variables used to estimate collapse height for a perfectly reinforced embankment (modified from Rowe and Soderman 1987a)

The bearing capacity q_u of the equivalent rigid footing of width b is given by

$$q_u = N_c s_{uo} + q_s \tag{3}$$

where q_s is a uniform surcharge pressure applied to the foundation soil surface outside the footing width. The bearing capacity factor N_c is obtained from Figure 1. Inspection of Figure 2 shows that the triangular edge of the embankment is providing a surcharge which would increase stability, and hence an estimate of q_s in terms of the pressure applied by this triangular distribution is required. Figure 3 shows the depth d to which the failure mechanism is expected to extend. The lateral extent of the plastic region involved in the collapse of a rigid footing extends a distance x from the footing, where x is approximately equal to the minimum of d, as obtained from Figure 3, and the actual thickness of the deposit, D, i.e.

$$x = \min(d, D) \tag{4}$$

Thus distributing the applied pressure due to the triangular distribution over a distance x gives

$$q_s = \frac{n\gamma(h^*)^2}{2x} \quad \text{for } x > nh^* \tag{5}$$

and

$$q_s = \frac{(2nh^* - x)\gamma h^*}{2nh^*} \quad \text{for } x < nh^* \tag{6}$$

This value may then be compared with the average applied pressure q_a due to the embankment over the width b:

$$q_a = \frac{\gamma\left[BH + n\left(H^2 - (h^*)^2\right)\right]}{b} \tag{7}$$

The maximum possible factor of safety (defined here as $FS = q_u/q_a$) that could be achieved for a given embankment geometry and soil profile under undrained conditions can be calculated directly from Equations 1–7. If the desired factor of safety for the proposed embankment is less than FS calculated in this manner, then reinforcement

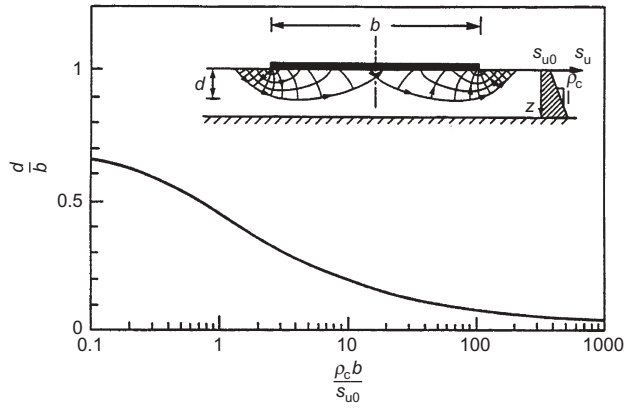

Figure 3. Effect of nonhomogeneity on depth of failure zone beneath a rough rigid footing (modified from Matar and Salencon 1977)

can potentially allow construction of the embankment to the desired height. If not, then either a lower factor of safety would have to be accepted (together with the use of reinforcement) or alternative measures (e.g. PVDs, stage loading, berms or the use of lightweight fill) would be needed in addition to the use of reinforcement.

The maximum possible factor of safety (FS) calculated above implicitly assumes that the reinforcement has sufficient strength and stiffness to develop the required reinforcement forces without breaking or excessive deformation. Having established that it is possible to build the embankment to the desired factor of safety, the next step (to be discussed in the following section) is to select reinforcement which has sufficient strength and stiffness to achieve the desired factor of safety.

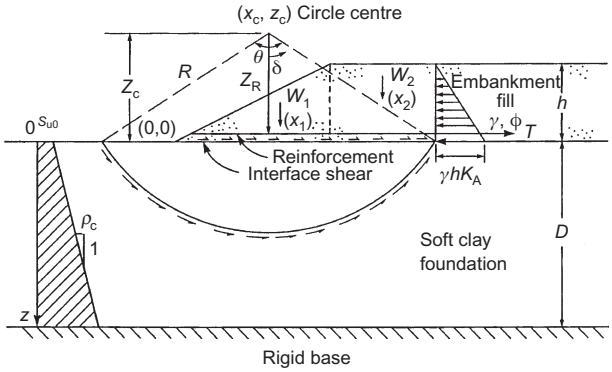

Figure 4. General arrangement of limit equilibrium method by Mylleville and Rowe (1988)

2.3. Limit equilibrium methods

Limit equilibrium methods have been used extensively to assess the short-term (undrained) stability of reinforced embankments constructed on soft foundation soils (e.g. Haliburton 1981; Ingold 1982; Jewell 1982; Milligan and LaRochelle 1984; Rowe and Soderman 1985a; Mylleville and Rowe 1988; Low *et al.* 1990; Holtz *et al.* 1997; Koerner 1997; Li and Rowe 2001a). These methods have been used to examine the equilibrium of the following mechanisms:

(1) bearing capacity failure of the foundation which involves the entire embankment;
(2) lateral sliding of a block along the embankment fill–reinforcement interface, foundation–reinforcement interface, or along a weak layer in the foundation soil; and
(3) a slip circle-type failure mechanism passing through the embankment fill and foundation soil.

The various methods are similar in that limiting equilibrium is established for the system of external forces acting on an assumed failure mass.

It is generally agreed that the reinforcement can be represented by an external restoring force acting on the failure mass. Historically, there has been debate regarding the inclination (orientation) and magnitude of this force. However, there is now strong evidence that the reinforcement force should be taken to act in its original horizontal orientation.

Mylleville and Rowe (1988) proposed a limit equilibrium method which is a modified version of a method by Jewell (1982). In this method, the failure surface in the foundation is approximated by a circular arc, and the embankment is modelled by a means of an equivalent surcharge pressure on the foundation and a horizontal thrust (due to earth pressure within the embankment), as illustrated in Figure 4.

The restoring force due to the reinforcement is assumed to act along the line of its original (horizontal) orientation, at the intersection of the failure surface and the reinforcement. In the following, it is assumed that the reinforcement is located within the fill material and not directly on top of the foundation. The procedure can be modified to consider the case where the reinforcement is directly on the foundation soil.

A commonly used limit equilibrium method considers moment equilibrium about the circle centre under consideration. The overturning moments are made up of two components, one being that due to the embankment fill weight contained within the slip circle and the other that due to a thrust force within the embankment fill itself. The thrust force tends to push the embankment fill outwards. The restoring moments are derived from the reinforcement and shear strength of the clay foundation along the assumed failure surface. A closed-form expression is used to compute the resisting moment due to the clay foundation and allows one to consider either a homogeneous deposit or a deposit where the shear strength varies with depth. Figure 4 shows the general arrangement of the limit equilibrium problem (taking the embankment toe as the origin of the coordinate system).

$$\text{Equilibrium ratio , ERAT} = \frac{\text{Restoring moments}}{\text{Overturning moments}} \tag{8a}$$

i.e.

$$\text{ERAT} = \frac{\text{MRR} + \text{MRSOIL}}{\text{MOFILL} + \text{MOPT}} \tag{8b}$$

where, for limit equilibrium, we require ERAT = 1, MRR = $Z_R T$ is the restoring moment due to limiting force developed in the reinforcement, $T = \min(T_1, T_2, T_3, T_4)$, and T_1, T_2, T_3, T_4 are defined as below:

(1) Sum of thrust force in fill and clay-fill interface shear, T_1:

$$T_1 = \tfrac{1}{2} K_A \gamma h^2 + \delta s_{uo} \left[x_c + R \sin\left(\frac{\theta}{2}\right) \right] \tag{9}$$

where δ = clay–fill interface adhesion factor; K_A = coefficient of active earth pressure.

(2) Pullout capacity of reinforcement, T_2:

$$T_2 = 2 \int_0^{x_c + R \sin(\theta/2)} \sigma_N \, dx \tag{10}$$

where σ_N = normal stress acting on the reinforcement

(3) Allowable reinforcement force governed by strength, T_3

(4) Allowable reinforcement force governed by allowable strain ε_a, T_4:

$$T_4 = J\varepsilon_a \tag{11}$$

where J is the secant stiffness of the reinforcement over the strain range $(0-\varepsilon_a)$, and

$$\text{MRSOIL} = \int_{-\theta/2}^{\theta/2} s_u(z) R^2 \, d\delta \tag{12a}$$

is the restoring moment due to the mobilized shear strength along the circular failure surface in the clay foundation, therefore

$$\text{MRSOIL} = s_{uo} R^2 \theta - \rho_c Z_c R^2 \theta + 2R^3 \rho_c \sin\left(\frac{\theta}{2}\right) \tag{12b}$$

$$s_u(z) = s_{uo} + (R\cos\delta - z_c)\rho_c \tag{12c}$$

MOFIILL = sum of overturning moments due to embankment fill self-weight applied to the clay foundation. (The embankment fill is subdivided into a number of regions to simplify computations). Therefore

$$\text{MOFILL} = W_1(x_1 - x_c) + W_2(x_2 - x_c) + \ldots = \sum_{i=1}^{nr} W_i(x_i - x_c) \tag{13}$$

where W_i = weight due to embankment fill of region i, x_i = centroid x coordinate of region i, $x_c = x$ coordinate of circle centre, $z_c = z$ coordinate of circle centre, and nr = number of regions.

MOPT = overturning moment due to horizontal thrust pressure (force) in the embankment fill, therefore

$$\text{MOPT} = \tfrac{1}{2} K_A \gamma h^2 \left(z_c - \frac{h}{3}\right) \tag{14}$$

The limit equilibrium method described above can be easily implemented in the form of a computer program, which can search for a slip circle giving the lowest equilibrium ratio for a given embankment. The maximum height to which an embankment can be constructed may be calculated by an iterative approach. If the soil strength is used and the lowest ERAT value is equal to unity, the corresponding height is the collapse height. Partial factors may be applied to the interface strength, pullout capacity and reinforcement strength as appropriate. When appropriate partial factors have been applied, one seeks reinforcement such that ERAT $\geqslant 1$.

2.4. Finite element methods

Methods of analysis such as limit equilibrium and plasticity solutions (previously described) provide no information about deformations or strains, which develop in the reinforcement for a given reinforced embankment. Reinforced embankments are a composite system consisting of three components: the foundation soil, the reinforcement, and the embankment fill. Their performance is highly dependent on deformations and on the interaction between these components.

The cost of constructing and monitoring full-scale field test embankments in order to assess the performance of various reinforcing schemes is sufficiently large that it is generally impractical. An alternative is to perform numerical simulations of 'embankment construction' using appropriate numerical models (Rowe and Soderman 1987b; Chai and Bergado 1993a; Hird *et al.* 1996; Li and Rowe 2001a) verified against what limited field cases are available.

The finite element method has proven to be a powerful technique for use in the evaluation of slope and embankment behaviour since its first use for this application by Clough and Woodward (1967). Numerous researchers have employed finite element techniques to interpret the field behaviour of reinforced embankments and to conduct sensitivity studies (e.g. Andrawes *et al.* 1980; Rowe 1982, 1984; Boutrop and Holtz 1983; Monnet *et al.* 1986; Duncan *et al.* 1987; Schaefer and Duncan 1988; Humphrey and Holtz 1989; Hird and Kwok 1990; Mylleville and Rowe 1991; Chai and Bergado 1993b; Litwinowicz *et al.* 1994; Rowe *et al.* 1996; Varadarajan *et al.* 1997; Rowe and Hinchberger 1998). These numerical models have incorporated soil models with different levels of sophistication including the hyperbolic elastic model (e.g. Andrawes *et al.* 1980), Mohr–Coulomb model (e.g. Rowe and Soderman 1985a), Cam-Clay model (e.g. Schaefer and Duncan 1988); Modified Cam-Clay model (e.g. Chai and Bergado 1993b; Rowe *et al.* 1996), and viscoplastic Elliptical Cap model (Rowe and Hinchberger 1998). A linear, bilinear or nonlinear bar model is commonly used to model reinforcement sheet (e.g. Rowe and Soderman 1985a; Hird and Kwok 1989; Bathurst *et al.* 1992). With newly developed fast scalar, parallel and vector computers, it has become feasible to use finite element models that are sufficiently sophisticated to model the essential characteristics of reinforced embankments on soft foundations, and to investigate time-dependent behaviour of reinforced embankments under a wide range of conditions (Li 2000).

The numerical models and techniques used should provide adequate predictive accuracy to capture the essential behavioral characteristics of the soil, the reinforcement and the soil–reinforcement interactions. The actual construction process can be simulated by turning on the gravity load of each layer (or lift) of embankment elements at a rate corresponding to the construction rate.

As noted earlier, the constitutive models for the soil used in analysing reinforced embankments may be subdivided into four categories: the nonlinear elastic (e.g. hyperbolic), elasto-perfectly-plastic, strain-hardening (e.g. cap model) and elasto-viscoplastic models. Nonlinear elastic models may provide acceptable results at low stress levels but cannot correctly model plastic failure and plastic strains within the soil mass. Thus these models will

give poor predictions of the behaviour of the foundation soil prior to embankment failure. Nonlinear elastoplastic models with a Mohr–Coulomb failure surface and non-associated flow rule are suitable to model the behaviour of typical granular soils used for embankment fill and for foundations that do not experience significant strain-hardening or viscous behaviour over the time period of interest. However, accurate prediction often requires consideration of the yielding behaviour of cohesive soils under embankment loading, and a critical state model (e.g. Modified Cam-Clay model) or Elliptical Cap model may be needed. Although some soil can be adequately modelled using Cam-Clay or Modified Cam-Clay, the Elliptical Cap model has greater flexibility for modeling embankment behaviour since it allows the shape of the yield envelope to be adjusted for the particular soil being considered.

Nonlinear elastoplastic models fully coupled with Biot consolidation theory (Biot 1941) have been widely used for consolidation analyses. The variation in the hydraulic conductivity of cohesive soils during loading and consolidation (Tavenas and Leroueil 1980) can be considered by using Taylor's equation (Taylor 1948), which correlates the hydraulic conductivity with the void ratio of soils.

Viscoplastic soil models are needed to model the time-dependent behaviour of reinforced embankments on rate-sensitive soft foundation soils (e.g. Rowe and Hinchberger 1998). Any such viscoplastic model should be able to capture the creep-induced excess pore pressure and strain-rate dependence of undrained shear strength.

If an embankment is reinforced using creep-insensitive reinforcement (e.g. some high-tensile stiffness PET geogrids), the reinforcement can be modelled using a one-dimensional bar element with a linear or nonlinear elastic constitutive relation. For creep-susceptible geosynthetic reinforcement (e.g. polyolefin geogrids), a nonlinear viscoelastic or viscoplastic model should be used to describe the creep and stress-relaxation behaviour of geosynthetic materials (e.g. Li and Rowe 2001b).

The interaction between the soil mass and reinforcement can be modelled by using interface elements which can have linear elastic deformations prior to slip and allow slippage between soil and reinforcement after the interface strength is reached. In general, a Mohr–Coulomb failure criterion is adequate to predict the failure of a soil–reinforcement interface, although cases have been reported where nonlinear (hyperbolic) models were considered necessary (Bathurst *et al.* 1992). Based on the authors' experience, a Mohr–Coulomb model has proven adequate for embankments with granular fills.

Reinforced embankments on foundation soils in which PVDs have been installed require special consideration. Strictly speaking, the analysis of a system involving discrete vertical drains should be conducted with a fully 3-D analysis, whereas most embankments are modelled for plane strain conditions. To avoid the need for a full 3-D analysis, some approximation is required to allow vertical drains to be reasonably modelled in a plane strain analysis. Both Li (2000) and Sharma and Bolton (2001) have shown that the techniques proposed by Hird *et al.* (1992, 1995) are suitable for matching a plane strain vertical drain system with an axisymmetric vertical drain system.

3. CASE HISTORIES

Numerous case studies have shown that the use of geosynthetic reinforcement typically reduces the cost of construction, increases the feasibility of construction, and increases the stability of embankments on poor foundation soils. However, it has also been reported that the field behaviour of reinforced embankments is significantly different from that expected based on the simplifications made in current design methods (e.g. Bassett and Yeo 1988; Duarte and Satterlee 1989; Fritzinger 1990; Litwinowicz *et al.* 1994). This section highlights the key findings based on the field behaviour reported in the literature, and represents a summary of a more detailed discussion by Rowe and Li (2001). The key issues are summarized in Table 1.

3.1. Benefits due to the use of reinforcement

The benefits of reinforcement in increasing embankment stability were clearly demonstrated by the Almere test embankment, where unreinforced and reinforced (tensile stiffness $J = 2000$ kN/m) granular fill sections were constructed on a 3.3 m thick organic clay foundation with an undrained shear strength of 8 kPa. The reinforced embankment experienced a relatively ductile failure at a height of 2.75 m, which is in remarkable contrast to the rapid failure of the unreinforced section at 1.75 m thickness. Rowe and Soderman (1984) demonstrated that both limit equilibrium and finite element analysis could capture the effect of the reinforcement on embankment stability. Bergado *et al.* (1994) and Loke *et al.* (1994) reported the field behaviour of two reinforced embankments constructed over soft Bangkok clay using two types of geosynthetic reinforcement. It has been shown that the tensile force mobilized in reinforcement increased the embankment stability after the foundation soil became plastic and reduced the lateral deformation of the foundation soil. The stiffer the reinforcement, the higher the embankment could be constructed.

It is evident from the field cases cited in Table 1 that the use of basal geosynthetic reinforcement can increase embankment stability and reduce deformations. The benefits arising from the use of geosynthetic reinforcement include the improvement of embankment behaviour, cost savings, an increase in the feasibility of embankment construction, and the elimination of stage construction in some cases.

3.2. Field reinforcement force and strain values

Current design methods for reinforced embankments are usually based on limit equilibrium analyses (e.g. Jewell 1982; Fowler and Koerner 1987; Leshchinsky 1987; Holtz *et al.* 1997). For embankments on soft cohesive deposits, the foundation soils are commonly assumed to respond in an undrained manner during embankment construction, and the critical time with respect to stability is typically considered to be at the end of construction.

It has been reported that the field behaviour of reinforced embankments can be significantly different from that anticipated in the design (Fowler and Edris Jr 1987; Hadj-Hamou and Bakeer 1991; Hashizume *et al.* 2000). The mobilized reinforcement force (or strain) is often only a small fraction of that predicted in design (Table 1). This either suggests that the current design methods may be too conservative, or it raises the question as to why the behaviour was not consistent with design expectations. These issues will be addressed in later sections of the paper.

3.3. Use of reinforcement and prefabricated vertical drains

The synergistic effects of the use of geosynthetic reinforcement and prefabricated vertical drains can improve the performance of embankments over soft foundations (Li and Rowe 1999b, 2001a). Lau and Cowland (2000) reported a case where neither reinforcement nor PVDs alone would have been sufficient to allow safe embankment construction to the design height. The combined use of both reinforcement and PVDs increased the short-term stability and made it feasible to construct this 4 m high embankment. The use of PVDs and control of the construction rate effectively reduced the excess pore pressures during construction and accelerated the dissipation of pore pressure after construction. The rate of strength gain of the soft clays due to partial consolidation arising from the presence of the prefabricated vertical drains was rapid and significant.

It has been also reported (Schimelfenyg *et al.* 1990) that the use of PVDs decreased the foundation heave and horizontal shear deformations during construction. In this case, the construction of a relatively high embankment over a foundation soil having extremely low undrained shear strength was achieved by the combined use of reinforcement and PVDs. These cases illustrate the importance of strength gain in the foundation due to partial consolidation during embankment construction where PVDs are used, and highlight the benefit that can arise from considering partial consolidation in design (as discussed in Section 6).

3.4. Factors contributing to low reinforcement strain

It is often reported that the mobilized reinforcement strain and force are significantly lower than expected in design. Varuso *et al.* (1999) showed that a reinforced levee designed with a factor of safety of 1 was stable and performed well. There are two factors contributing to this observation. First, the design was based on undrained shear strength measured using unconsolidated-undrained tests, which typically underestimate the actual undrained shear strength (due to disturbance). Second, there was a substantial increase in shear strength of the foundation soil during construction due to partial consolidation during construction, which increased the levee stability relative to that assumed in design.

Partial consolidation, occurring during construction over foundations improved by the installation of vertical drains, can result in mobilized reinforcement strains well below the design value (Fritzinger 1990). Chai and Bergado (1993b) reported the case of an 8.5 m-high reinforced embankment on soft Malaysian Muar clay where the reinforcement was not fully mobilized owing to the strength gain of the foundation resulting from the installation of PVDs.

The cases examined herein have shown that the observed reinforcement strain and force are usually less than the design values for a required factor of safety, or the values are less than predicted for equilibrium assuming the undrained strength of the soil has been fully mobilized. This can be attributed to three primary factors. First, current design methods conservatively assume undrained conditions for the foundation soils during embankment construction. However, in reality, significant partial consolidation can occur when the soil is overconsolidated during early stages of loading (Leroueil *et al.* 1978; Li and Rowe 1999a; Leroueil and Rowe 2001), and the consequent beneficial effect of the partial consolidation on stability is enhanced by the presence of embankment reinforcement (Li and Rowe 1999a).

The second source of conservatism arises from the selection of undrained shear strength values for the foundation soils. Owing to the uncertainty associated with the in-situ operational shear strength of foundation soils, the design strength is often conservatively selected as a lower-bound fit to the data from in-situ and laboratory tests rather than the expected value based on these same data. The third factor contributing to the mobilization of reinforcement strains lower than the design value is that the embankment is usually designed with a required global factor of safety greater than unity in conventional working stress design or using factored foundation strength in limit state design. Thus it is to be expected that, under working conditions, the mobilized reinforcement strain and force should be lower than the design values unless the shear strength of the foundation has been overestimated in the design.

Finite element analyses (Rowe and Li 1999; Li and Rowe 2001b) have demonstrated that the magnitude of reinforcement strain at working conditions typically ranges between 1% and 3%, which is consistent with many field observations and is substantially lower than the typical design strain of 5%.

3.5. The effect of construction rate and stage construction

Owing to the low undrained shear strength of very soft soils, it is often essential to allow the dissipation of excess pore pressure during embankment construction. For example, control of the rate of construction is important in maintaining the short-term stability of embankments over peat. Rowe and Soderman (1985b) recommended that the construction rate should be slow enough to ensure that the pore pressure parameter, B_{max}, remain below 0.34 (where $B_{max} = \Delta u/\Delta\sigma_v$, and Δu is the maximum excess pore pressure generated by a change in vertical total stress $\Delta\sigma_v$). In the Hubrey Road embankment case, this recommendation was not followed at one section, and a failure

Table 1. Summary of case histories of reinforced embankments

	H (m)	Foundation soils	Reinforcement	Performance	References
Benefits from the use of geosynthetic reinforcement	2.75	3.3 m thick organic clay with s_u = 8 kPa	1 layer of PET W-GT with J = 2000 kN/m	Use of geotextile reinforced increased failure height by 57%. Reinforcement reduced plastic deformations of foundation soil	Rowe and Soderman (1984)
	6.6	2.74–5.18 m thick soft organic silty clay overlying sand layers; s_u = 8–11 kPa	6 layers of HDPE uniaxial GG with T_{ult} = 80 kN/m	Significant savings; elimination of stage construction; excellent performance due to combined use of reinforcement and PVDs	Lockett and Mattox (1987)[a]
	Emb. A 4.2 Emb. B 6	8 m thick soft Bangkok clay with s_u = 15–30 kPa underlying a 2 m crust with s_u = 20–40 kPa	Emb. A having 4 layers NW-GT with T_{ult} = 8–18 kN/m; Emb. B having 1 layer of W-GT with T_{ult} = 200 kN/m	Use of reinforcement increased embankment failure height; higher strength and stiffness gave better performance	Bergado *et al.* (1994) Loke *et al.* (1994)
	5.5	4 m thick organic clay with LL = 56% and PL = 32% overlying 13.5 m high-plasticity organic clay	3-layer uniaxial GG with T_{ult} = 80 kN/m and $J_{5\%}$ = 1080 kN/m	Both geogrid reinforcement and stage construction increased factor of safety. Measured pore pressures were less than predicted	Mattox and Fugua (1995)[b]
Observed behaviour vs. design expectation	3.8	Low plasticity organic silt overlying high plastic clay with s_u = 7–22 kPa	1 layer of W-GT with T_{ult} = 664 kN/m and $J_{5\%}$ = 5950 kN/m	Range of geotextile strains and loads measured in field significantly less than values predicted in design	Fowler and Edris Jr (1987)
	3.1	Extremely soft to soft thick clay deposits with an average s_u = 7 kPa for the first 6 m soils	2 layers of HPDE uniaxial GG with T_{ult} = 80 kN/m and $J_{5\%}$ = 1080 kN/m	Mobilized reinforcement force only 73% of design strength	Hadj-Hamou and Bakeer (1991)
	13.2	15 m thick soft ground	1 layer of GG with T_{req} = 700 kN/m	Observed reinforcement strain and force less than design values	Hashizume *et al.* (2000)
Combined use of reinforcement and PVDs	4.0	6–12 m thick river mud and alluvial clay deposits with s_u = 7.5–16 kPa	1 layer of W-GT with T_{req} = 200 kN/m	Consolidation during construction and strength gain were significant	Lau and Cowland (2000)[a]
	5.0	1.2–5.2 m thick organic clay with s_u = 1–12 kPa and w_n = 105%	1 layer of PET W-GT with T_{ult} = 880 kN/m and $J_{5\%}$ = 8800 kN/m	Yse of PVDs decreased both foundation shear deformations and reinforcement strains	Schimelfenyg *et al.* (1990)[a,b]
Factors contributing to low mobilization of reinforcement strains and forces	3.7	25 m organic silty clays, very soft to medium consistency with high water content and s_u = 7–30 kPa	Three sections: (a) 1 layer of GT; (b) 1 layer of uniaxial GG; (c) 2 layers of GG Each section has total reinforcing force of $T_{5\%}$ = 85 kN/m	Strength gain during and shortly after construction 50–135%. Resulted in low mobilized reinforcement strain	Varuso *et al.* (1999)
	6.0	7.5–30.5 m thick soft and highly compressible silts and clays with s_u = 4.8–9.4 kPa	1 layer of PET W-GT with T_{ult} = 260 kN/m and J = 3300 kN/m	Consolidation during construction resulted in observed reinforcement strains below design strain of 5%	Fritzinger (1990)[a,b]
	8.5	2 m crust overlying very soft silty clay with w_n = 80–105% and s_u = 10–30 kPa	2 layers of GG with T_{ult} = 110 kN/m	Stage construction and PVDs increased embankment stability and decreased reinforcement strain	Chai and Bergado (1993b)[a,b]

Importance of controlled construction rates	1.3–1.7	1.8–1.9 m of fibrous peat with w_n = 250–700% overlying 2.6–3 m very soft organic silt with w_n = 250–480% and s_u = 4–12 kPa	1 layer of PP biaxial GG with T_{ult} = 19 kN/m and $J_{5\%}$ = 280 kN/m	Control of construction rate vital to maintain embankment stability	Rowe and Mylleville (1996)[b]
	2.9	6–7 m very soft organic marine clay with w_n = 90–400% and s_u = 1.4–9.6 kPa	2-layer PET W-GT with T_{ult} = 730 kN/m, J = 3500 kN/m, and T_{ult} = 438 kN/m, J = 5940 kN/m	Strength gain of soils due to stage construction permitted construction to design height without exceeding design reinforcement strain	Volk *et al.* (1994)[a,b]
	4.3	9–15 m very soft to soft lacustrine clayey silt with s_u = 10–19 kPa	2 layers of PET W-GT with T_{ult} = 200 kN/m	Use of high-strength GT and stage construction made it feasible to construct embankment within project schedule	Shimel and Gertje (1997)
Reinforced embankment constructed over rate-sensitive soils	8.2	Rate-sensitive soft organic clayey silt deposits, w_n = 40–110%, LL = 42–76%, LI >1 and s_{uvane} = 22–40 kN/m	PET W-GT with T_{ult} = 216 kN/m and $J_{5\%}$ = 1466 kN/m	Soil deformations and excess pore pressure increased after EOC owing to creep of foundation soils. Vane shear strength overestimated strength of this rate-sensitive soil	Rowe *et al.* (1995) Rowe and Hinchberger (1998)
Increase of reinforcement strain after construction	2.8	4–10 m very soft/soft organic marine silty clay with w_n = 40–120%, LI = 1.5–2.5 and s_u = 5–12 kPa.	Two sections, one with 1 layer of HPDE GG ($J_{3\%}$ = 3500 kN/m) with 1 layer of the other PET-GG ($J_{3\%}$ = 2100 kN/m)	During post-construction periods, creep of HPDE reinforcement was significant and creep of PET reinforcement was insignificant	Litwinowicz *et al.* (1994)
	7	Soft clay overlying peat overlying soft clay with total thickness of 4.5 m	1 layer of HPDE GG with T_{ult} = 79 kN/m and $J_{2\%}$ = 1094 kN/m	Both reinforcement strain and force increased significantly during 13 months after EOC	Bassett and Yeo (1988)[a]
Reinforced embankments over peat	1–1.5	Peat with w_n = 445–785%	Two sections: Section A with W-GT (T_{ult} = 41 kN/m) and Section B with W-GT (T_{ult} = 178 kN/m)	Reinforcement reduced shear deformations and had no effect on consolidation settlements. Effective stress analyses resulted in good agreement with field data	Rowe *et al.* (1984a, 1984b)
	5.8	1.5–3 m peat with w_n = 150–319% overlying 1–2 m clay with w_n = 44–86% and s_u = 40–60 kPa	2 layers of W-GT with T_{ult} = 120 kN/m and J = 600–1200 kN/m	Use of reinforcement made it feasible to construct this embankment. Mobilized reinforcement force about one third of design value	Matichard *et al.* (1994)
	6.0	1.2–11.3 m thick peat with w_n = 260–400%	5 layers of GG: 1 layer with T_{ult} = 18 kN/m and 4 layers with T_{ult} = 108 kN/m	Reinforcement layers made construction possible and resulted in rigid-footing-like behaviour of embankment	Oikawa *et al.* (1996)[b]
	5.0	2.5 m of peat with w_n = 92–581% overlying 2.5–5.5 m of soft clay with w_n = 10–60% and s_u = 5–10 kPa	1 layer of HPDE GG with design strength of 61 kN/m	Use of reinforcement eliminated need for removing peat and reduced construction time by half	Kerr *et al.* (2001)

[a]With PVDs; [b]with stage construction.

H = embankment height; GT = geotextile; GG = geogrid; W = woven; NW = nonwoven; PET = polyester; PE = polyethylene; HDPE = high-density polyethylene.

occurred when the excess pore pressure parameter B_{max} was 0.7 (Rowe and Mylleville 1996).

Stage construction is often used to achieve sufficient strength gain of the foundation soil to allow final construction of embankments to the design height. The combined use of embankment reinforcement and stage construction can be very efficient since the beneficial effect of consolidation is enhanced by the use of reinforcement (Rowe and Li 1999; Li and Rowe 2001a; see Section 5). Field examples include the use of two layers of reinforcement combined with stage construction to allow the construction of a 2.9 m-high embankment on a very soft organic soil as reported by Volk *et al.* (1994). Shimel and Gertje (1997) also reported that the use of high-strength reinforcement in combination with stage construction allowed timely construction of a 4.3 m-high embankment over a soft foundation within the project schedule. The rate of embankment construction was controlled to maintain stability by monitoring pore pressures and horizontal displacements during fill placement.

The field cases cited herein show that the control of the construction rate to allow the dissipation of excess pore pressures during embankment construction can be a useful approach for ensuring embankment stability over soft foundations, and that partial consolidation should be considered in design, especially when both reinforcement and PVDs are used.

3.6. Reinforced embankments on rate-sensitive soils

A fully instrumented embankment with both reinforced and unreinforced sections was constructed over a soft compressible clayey silt deposit in Sackville, New Brunswick (Rowe *et al.* 1995, 2001; Rowe and Hinchberger 1998). The natural water content ranged from 40% to 70%, the liquid limit from 42% to 76%, and the plastic limit from 15% to 23%. The liquidity index exceeded unity at depths from 1 to 6 m.

The field monitoring indicated that the embankment behaved elastically up to about 2.4 m fill thickness, and that there were significant plastic deformations in the soil during the construction of the embankment from 5 to 5.7 m. The unreinforced embankment failure height was about 6.1 m (Rowe *et al.* 2001), and the reinforced embankment failure height was 8.2 m. Rowe *et al.* (1995) described the failure of the Sackville test embankment as a viscous type of failure. During the construction, for fill thicknesses greater than 2.4 m, the recorded reinforcement strain and embankment deformations increased significantly with time after each embankment lift was placed. The reported behaviour (Rowe *et al.* 1995) has provided field data that can be used to validate a viscoplastic soil model for rate-sensitive foundation soils under embankment loadings (Rowe and Hinchberger 1998). The calculated reinforcement strains were shown to agree with the measured strains during embankment construction (Figure 5), and the numerical model closely predicted the time-dependent increase in reinforcement strain.

The viscoplastic model successfully predicted the creep-induced excess pore pressure during the stoppage at the fill thickness of 5.7 m (Figure 6). The deformations of

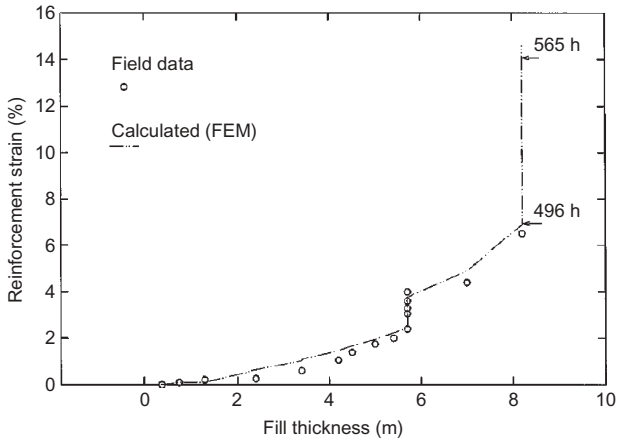

Figure 5. Calculated and measured reinforcement strains against fill thickness (8.8 m from embankment toe) (modified from Rowe and Hinchberger 1998)

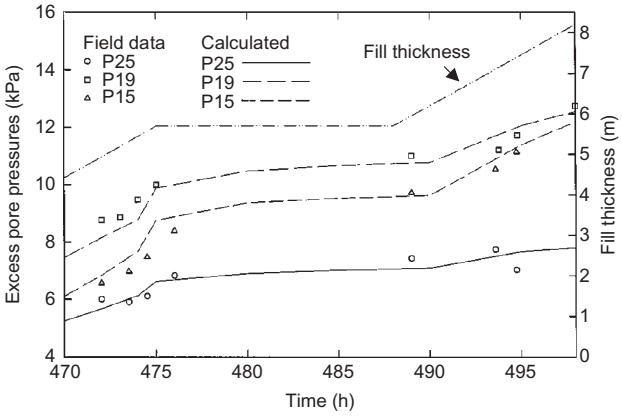

Figure 6. Excess pore pressures at piezometers 15, 19 and 25 during constant embankment loads (5.7 m fill thickness) (modified from Rowe and Hinchberger 1998)

Sackville soils were influenced by the viscoplastic characteristics of the rate-sensitive soil, and time-dependent deformations were also generally well predicted by the model (Figure 7).

The Sackville reinforced embankment case (Rowe *et al.* 1995) has also shown that the field vane shear strength may overestimate the operational strength rate-sensitive soils even after application of the Bjerrum correction. Subsequently it has been shown that the undrained shear strength correction factor proposed by Li and Rowe (2002) can be used to estimate the operational strength of rate-sensitive soils under embankment loadings (Section 8).

3.7. The increase of reinforcement strain after construction

Litwinowicz *et al.* (1994) reported on a 2.8 m-high embankment constructed on 4–10 m deep very soft to soft marine clay. One section was reinforced with an HDPE geogrid and the other was reinforced using a polyester geogrid. The maximum strain in the HDPE geogrid increased by 100% after the end of construction while the strain in the PET geogrid increased slightly. The increase of HPDE geogrid strain at constant embankment load was

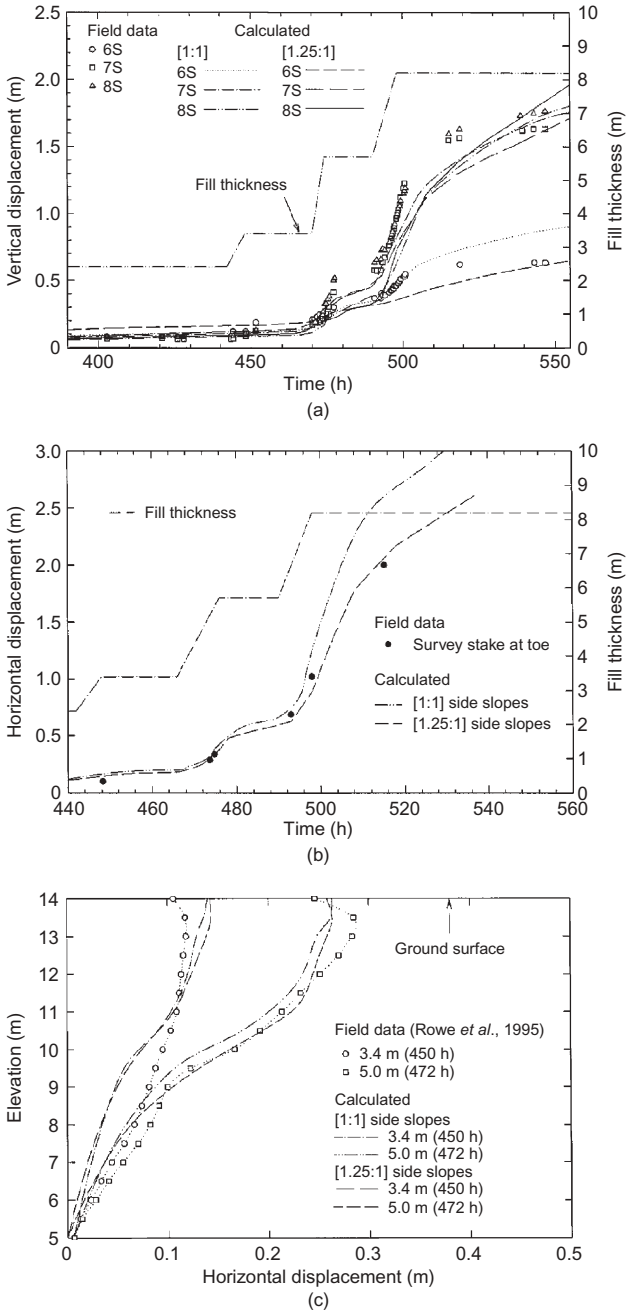

Figure 7. Comparison of calculated and measured vertical and horizontal deformations (modified from Rowe and Hinchberger 1998): (a) vertical displacement (m) with time (h) at settlement plates; (b) horizontal displacements (m) at embankment toe; (c) relative horizontal displacement profile (m) at inclinometer 231

attributed mainly to creep of the geogrid. However, the magnitude of the increase (i.e. 0.5%) was significantly less than the 2.5% predicted from isochronous creep curves. This may be due to the fact that creep of the reinforcement can be limited by the soil under working conditions (Li and Rowe 2001b).

Bassett and Yeo (1988) also reported a significant increase of strains in reinforcement after embankment construction. In this case, a 7 m-high trial embankment reinforced with a uniaxial HDPE geogrid was constructed across a 4.5 m thickness of soft clay/peat/soft clay installed with vertical drains. Following construction, the strain increased by 50% (i.e. from 2% to 3%) and the geogrid force increased by 10%. The increase of reinforcement strain and force after the end of construction was contrary to design expectations. Creep of both the reinforcement and foundation soil can increase the reinforcement strain, as shown in Sections 8 and 9.

3.8. Embankments over peat

Geosynthetic reinforcement has been successfully used in the construction of embankments over peat foundations. Rowe *et al.* (1984a, 1984b) reported that the Bloomington road embankment with 5.9 m fill thickness was constructed over a highly compressible peat deposit using geotextile reinforcement. The thickness of the peat in this deposit varied between 5 m and 7.6 m. The average water content of the peat was 445% and 785% at the two investigated Sections A and B. Section A was reinforced by a woven geotextile with an ultimate wide-width tensile strength $T_{ult} = 41$ kN/m, and Section B was reinforced with another woven geotextile with $T_{ult} = 178$ kN/m. The high tensile stiffness geotextile used in Section B reduced lateral movements. In the analysis of embankment performance, the use of effective deformation and strength parameters (combined with pore pressures) provided the best agreement between calculated and observed behaviour.

In the case reported by Matichard *et al.* (1994), the increase of effective stress in the peat due to the relative rapid dissipation of the excess pore pressures during embankment construction resulted in reinforcement strains significantly lower than the design value.

Oikawa *et al.* (1996) reported that a relative high embankment was successfully constructed over a peat foundation using multi-layers of geosynthetic reinforcement. The reinforcement layers resulted in a rigid-footing-like behaviour of the embankment. The relatively small shear deformations of the peat foundation during and after the fill placement were attributed to the use of reinforcement and the rapid consolidation of the peat.

True peats (as opposed to organic clays) typically have a high natural water content (50–2000%), high void ratio (5 to 15 but may be up to 25), and high compressibility. The hydraulic conductivity of peat is usually high but reduces significantly as the peat compresses. Since the porous nature of peat usually allows partial dissipation of excess pore pressure during construction for typical rates of construction, undrained bearing capacity failures are rare for peat deposits underlain by a firm foundation. Failures of embankments over peats are usually caused by excessive shear deformations of the embankment rather than a definite sliding surface. Effective stress analyses, rather than total stress analyses based on the 'undrained shear strength', are applicable to embankments over peat foundations and give good predictions (Rowe *et al.* 1984b). Undrained shear strengths reported for fibrous peat should be viewed with suspicion (Landva 1980).

3.9. Summary

Numerous embankments have been successfully constructed on soft foundations using geosynthetics. Geosynthetic reinforcement and/or PVDs allowed construction on these difficult foundation soils within prescribed construction schedules and performance criteria.

Reinforcement increased the factor of safety against rotational failure and served to maintain the structural integrity of the embankments. The bearing capacity of the foundation soil was also increased by the use of reinforcement. The reinforced embankment failure height is usually greater than that calculated based on classical bearing capacity theory using the Prandtl solution (Prandtl 1920) for a strip footing on a deep homogeneous clay layer (i.e. $H_f = 5.14s_u$), owing to either a significant increase in undrained strength with depth in foundation soils or/and a firm stratum at relatively shallow depth beneath the soft layer. Field data have shown that the use of high tensile strength, high tensile stiffness geosynthetics effectively reduced the movements at ground level, minimized lateral spreading, and reducing differential consolidation settlements.

To reach a design grade it is sometimes necessary to combine reinforcement with stage construction so that the foundation soil can have sufficient strength gain for the final embankment load. It has been shown that the effect of strength gain of foundation soils due to partial consolidation is enhanced by the use of geosynthetic reinforcement. At typical construction rates, partial consolidation can be significant when the soil is initially overconsolidated, when PVDs are installed, or when the foundation includes a fibrous peat layer. The consequent strength gain in the foundation can effectively reduce reinforcement strain developed at the end of construction. The magnitudes of the mobilized reinforcement strain and force have been found to be significantly less than the values used or expected with current design methods in numerous cases where the embankments were constructed over conventional soft soils. This is attributed mainly to the conservative assumption of undrained conditions used in most current design methods combined with conservative assumptions associated with soil strength. The behaviour of a number of reinforced embankments indicates that the assumption of undrained conditions may often be too conservative, and that a design method allowing for the effects of partial consolidation could be used for the reinforced embankments.

Reinforced embankments constructed on rate-sensitive soils require special care. For such foundation soils, the most critical time with respect to embankment stability may be at some time after the end of construction rather than during construction. Thus, the reinforcement strain and force can increase substantially with time owing to the creep of the foundation soils. Another factor contributing to the time-dependent behaviour of reinforced embankments is the viscous behaviour of geosynthetics, especially those made of high-density polyethylene and polypropylene. In these cases, the reinforcement strains increase with time owing to creep of geosynthetics under constant embankment load. There is a paucity of data showing the stress relaxation of reinforcement after construction. This is considered to be because the post-construction horizontal deformations of foundation soils resulting from creep and consolidation deformations of foundation soils give rise to an increase in reinforcement force that can offset the stress relaxation in reinforcement.

4. UNDRAINED BEHAVIOUR OF REINFORCED EMBANKMENTS

4.1. Background

Previous studies (e.g. Rowe and Soderman 1985a, 1987b; Rowe and Mylleville 1989; Hird and Kwok 1990) provide significant insights into the undrained behaviour of reinforced embankments over soft clay. For example, Rowe and Soderman (1985a, 1987b) have shown that the embankment failure height increases substantially with reinforcement axial stiffness when the undrained shear strength of foundation soils increases with depth. They also showed that the reinforcement strain developed at embankment failure is a function of shear strength and tensile stiffness of the foundation soil and the geometry of the embankment–foundation system. Based on finite element parametric studies, Hird and Kwok (1990) have shown that reinforcement with sufficient stiffness and strength can significantly reduce the undrained displacement within the foundation (Figure 8), and that the benefit of increasing reinforcement stiffness diminishes for very stiff reinforcement. This is consistent with the findings reported by Rowe and Li (1999) based on analyses of partially drained conditions.

For an unreinforced embankment, the collapse height of the embankment simply corresponds to the height at which the soil shear strength is fully mobilized along a potential failure surface. This may also be the case for an extremely heavily reinforced embankment (i.e. one behaving as a rigid footing, as previously discussed). However, for most reinforced embankments, collapse involves failure of both the soil and some aspect of the soil–reinforcement system. The latter may involve (a) failure of reinforcement, (b) failure of the soil–reinforcement interfaces, or (c) failure to control deformations due to issues of strain compatibility (controlled by the relative moduli of the soil and reinforcement). The concepts of net embankment height (defined as fill thickness minus maximum vertical deflection) and allowable compatible reinforcement strain were introduced by Rowe and Soderman (1985a, 1987b) to account for failure due to excessive displacements before the reinforcement reaches its ultimate tensile strain or pullout occurs. For example, Figure 9 shows both net embankment height plotted against the fill thickness and the maximum reinforcement strain for an embankment constructed quickly on a soft clayey foundation. The failure of this reinforced embankment due to excessive subsidence occurred at a fill thickness equal to 2.4 m at a reinforcement strain of 5.2%. Most geosynthetic products can sustain strains well above 5.2% before they reach tensile failure (Industrial Fabrics Association

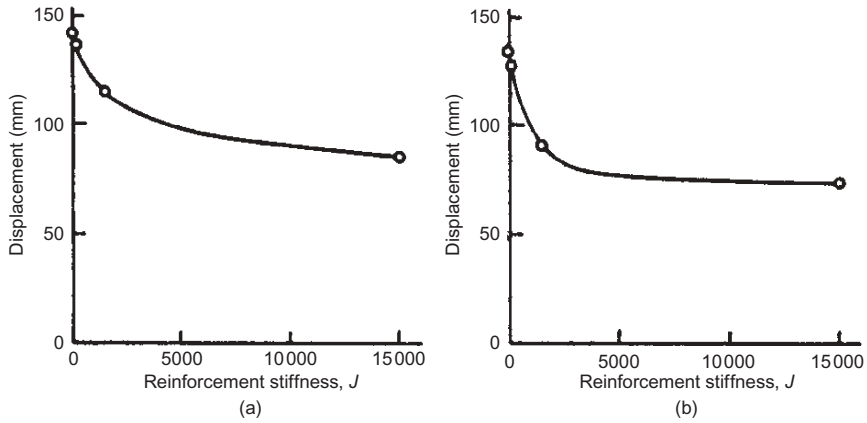

Figure 8. Effect of reinforcement tensile stiffness, J, on foundation deformations: (a) maximum settlement of foundation surface; (b) maximum horizontal displacement of foundation surface (after Hird and Kwok 1990)

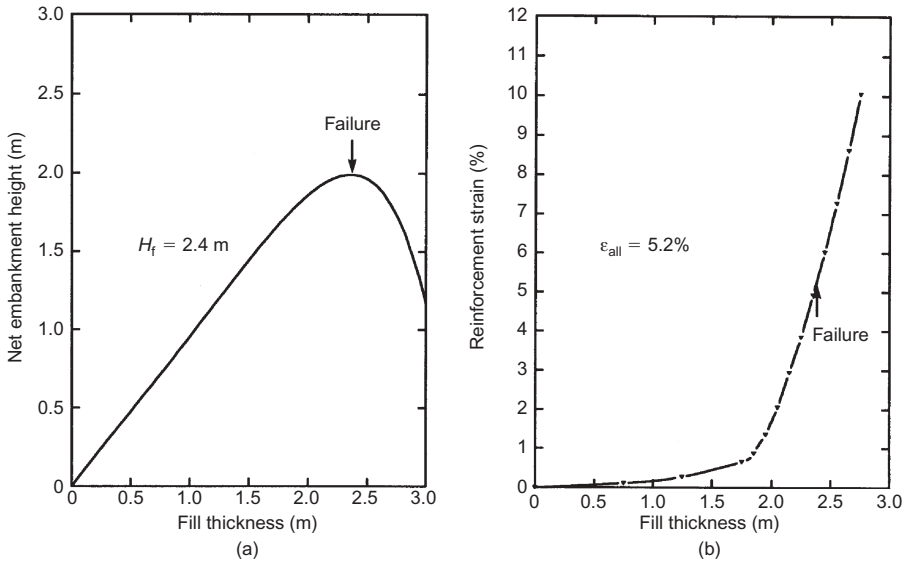

Figure 9. (a) Maximum net embankment height and (b) allowable reinforcement strain on soil with $s_{uo} = 3.8$ kPa and $\rho_c = 1.5$ kPa/m and reinforcement with $J = 600$ kN/m (after Hinchberger and Rowe 2003)

International 2004). Placement of fill beyond a thickness of 2.4 m for this embankment only degraded embankment performance without increasing the net embankment height (Figure 9a). Thus it is important to define an allowable 'compatible' reinforcement strain corresponding to the failure thickness of a reinforced embankment. A second allowable strain will be related to the reinforcement strength. The lower of these two strains will govern the design.

The allowable 'compatible' reinforcement strain will be discussed in the following subsections. If an embankment has a reinforcement with a tensile stiffness so small that negligible load is developed in the geosynthetic when a failure mechanism develops, one would expect the strains just prior to failure and the failure height of the reinforced embankment to be the same as those corresponding to failure of a similar unreinforced embankment. The maximum strain that would occur in this geosynthetic just prior to this failure is referred to as the 'allowable compatible strain' (Rowe and Soderman 1985a).

For reinforced embankments, the construction sequence may have a significant effect on the deformations of the foundation soil, based on the analyses reported by Rowe (1982) and Borges and Cardoso (1998). It has been found that, for each embankment fill lift, a fill placement sequence from the embankment toe to the embankment centre is favorable to reducing foundation horizontal deformations. However, the magnitude and distribution of reinforcement strains are independent of construction sequence, based on the analyses of Hinchberger (1996).

4.2. Soils with uniform undrained shear strength with depth

Rowe and Soderman (1985a) conducted an extensive finite element study to establish the allowable compatible strain for reinforced embankments on soils with uniform undrained shear strength. It was found that the compatible reinforcement strain developed prior to embankment failure was a function of the ratio of the thickness of the soft deposit, D, over the embankment width B, the ratio of the

undrained shear strength s_u over the undrained modulus of the soft foundation soil, and the ratio of $\gamma_f H_c/s_u$ (where γ_f = the bulk unit weight of the embankment fill and H_c = the height of an unreinforced embankment at collapse). Figure 10 shows the variation of allowable compatible strain with the dimensionless parameter, Ω, defined as:

$$\Omega = \left(\frac{\gamma_f H_c}{s_u}\right)\left(\frac{s_u}{E_u}\right)\left(\frac{D}{B}\right)_e^2 \quad (15)$$

where $(D/B)_e$ is the ratio of the effective depth of the deposit to the crest width, and

$$\left(\frac{D}{B}\right)_e = 0.2,\ D/B < 0.2 \quad (16a)$$

$$\left(\frac{D}{B}\right)_e = \frac{D}{B},\ 0.2 \leqslant D/B \leqslant 0.42 \quad (16b)$$

$$\left(\frac{D}{B}\right)_e = 0.84 - \frac{D}{B},\ 0.42 \leqslant D/B \leqslant 0.84 \quad (16c)$$

$$\left(\frac{D}{B}\right)_e = 0,\ 0.84 \leqslant D/B \quad (16d)$$

Thus in a limit equilibrium analysis of a reinforced embankment, the tensile force in the reinforcement, T, contributing to the restoring moment should not exceed the force that can be developed at the allowable compatible strain (i.e. $T = J\varepsilon_a$, where J is the secant tensile stiffness of the reinforcement over the strain range $0-\varepsilon_a$). For reinforced embankments on a deep uniform foundation soil ($D/B > 0.84$), the value of ε_a is zero and hence $T = 0$ (Figure 10). This implies that the reinforcement has no effect on deep-seated stability, and is consistent with the fact that the bearing capacity of a rough rigid footing ($\sim$ a reinforced embankment) on a deep uniform cohesive layer is identical to that of a smooth flexible footing ($\sim$ an unreinforced embankment) at $q_u = 5.14s_u$ for both cases. It should be noted that when using Equation 15 it is not conservative to underestimate the undrained modulus of the soft foundation soil, since a lower value of E_u corresponds to a high value of ε_a, which in turn gives a high reinforcement force T.

4.3. Soils whose strength increases with depth

As is shown in the previous subsection, when the strength of the foundation is uniform with depth the effectiveness of reinforcement is highly dependent on the geometry of the embankment relative to the layer depth. For layers with depths in excess of 0.5 times the embankment crest width, the contribution of even high tensile stiffness reinforcement to stability may be quite small. However, the effect of reinforcement is highly dependent on the reinforcement stiffness and the rate of the increase in undrained shear strength of the foundation with depth.

Finite element results show that the use of reinforcement changes the failure mechanism (Rowe and Soderman 1987b). In this example, the slip surface for the unreinforced embankment was relatively shallow (2 m below the ground surface for this case) owing to the lower strength in the upper layer foundation soils. However, the inclusion of basal reinforcement forces the collapse mechanism (i.e. the slip surface) down into the stronger soil at depth. In fact, the use of reinforcement with $J = 4000$ kN/m moves the edge of the slip surface from near the shoulder to near the centreline of the embankment and forces it from a depth of 2 m to a depth of 8.5 m (Figure 11). Thus, the mobilization of the higher soil strength at depth and the tensile resistance force in reinforcement results in a significant increase of embankment failure height.

For reinforced embankments over soft foundations, it is important to consider deformations in any assessment of embankment failure, and this is a function of reinforcement stiffness. For example, Figure 12 shows the net fill height above original ground level against the fill thickness. For the unreinforced embankment, the maximum net fill height is about 3 m and corresponds to the onset of contiguous plasticity in the foundation soil. In this case the failure and collapse height are the same, and the net fill height at the onset of collapse is only slightly less than the fill thickness. However, for the reinforced embankments, the maximum net fill height depends on the

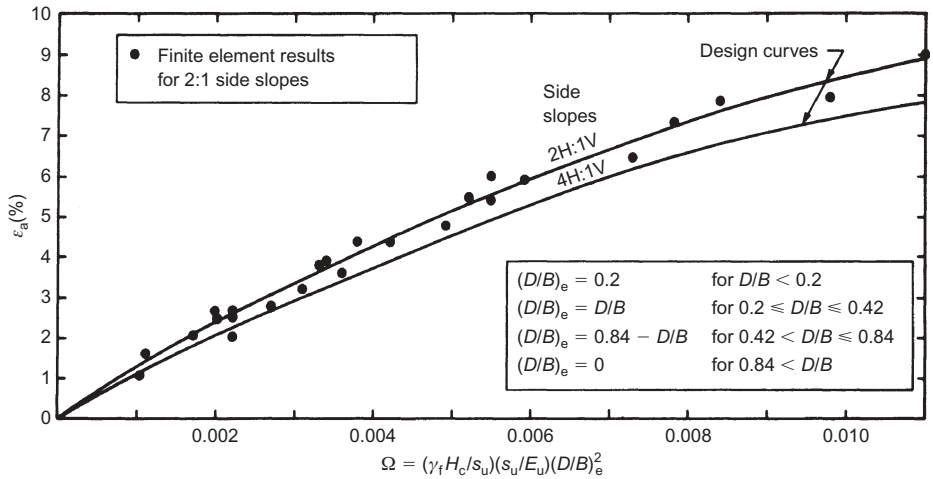

Figure 10. Variation of allowable compatible strain ε_a with dimensionless parameter Ω modified from Rowe and Soderman 1985a)

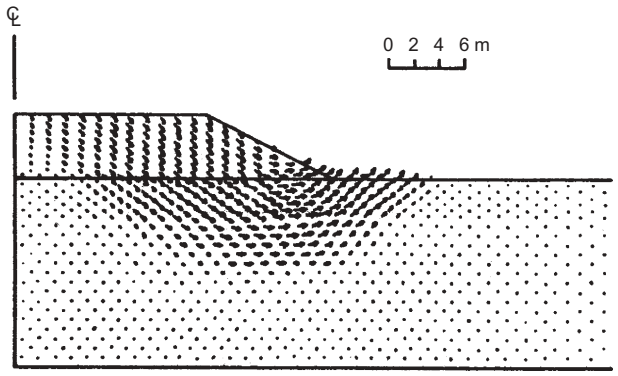

Figure 11. Velocity field at collapse for reinforced embankment ($J = 4000$ kN/m) on foundation soil with $s_{uo} = 7.69$ kPa and $\rho_c = 1.54$ kPa (after Rowe and Soderman 1987b)

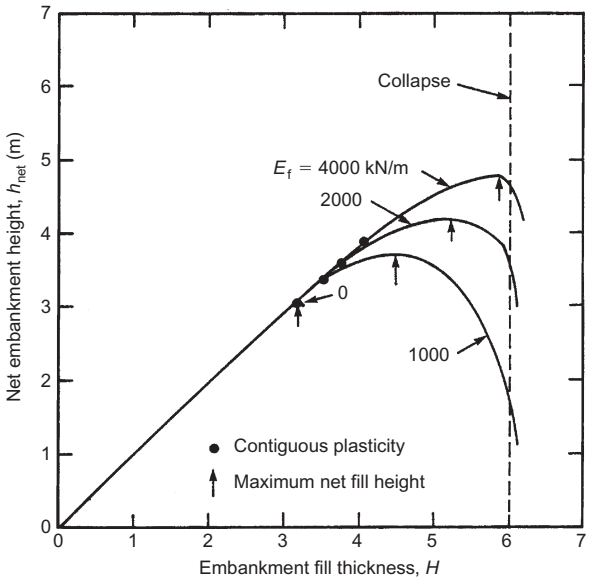

Figure 12. Net embankment height against fill thickness for various reinforcement tensile stiffness values (after Rowe and Soderman 1987b)

reinforcement tensile stiffness. Any attempt to place additional fill after attaining this maximum height will result in the loss of net height. The maximum height corresponds to the failure height of the embankment and is directly related to the reinforcement tensile stiffness for a given soil profile. The addition of fill will finally cause collapse of the reinforced embankment. The collapse load is independent of reinforcement stiffness (i.e. 120 kPa for this case).

The increase in fill thickness arises from three factors:

(1) the increase in geosynthetic tensile stiffness;
(2) the rate of increase in soil strength with depth; and
(3) the strength of the foundation–reinforcement interface.

Generally, the greater the increase in strength with depth, the greater the effect of increasing the reinforcement stiffness (Figure 13; Rowe and Soderman 1987b). For a strength increase with depth of 2 kPa/m, increases in the

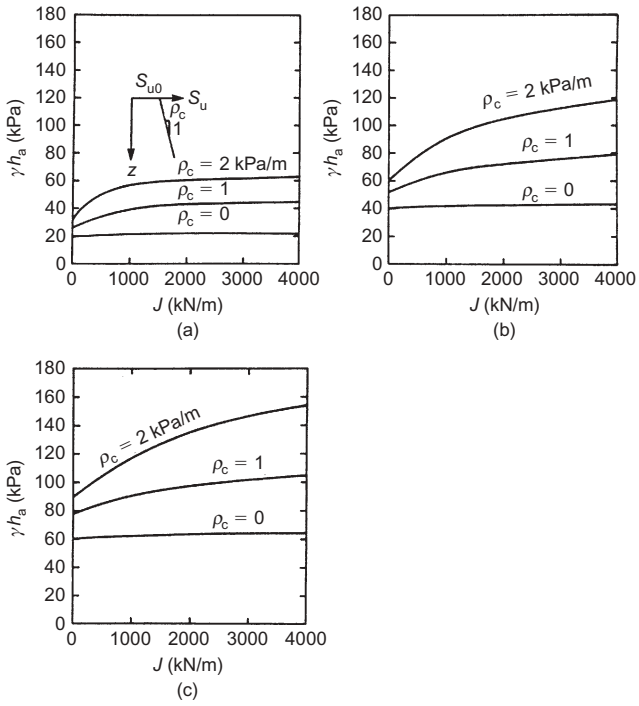

Figure 13. Allowable pressures, γh_a (based on FS = 1.3) against tensile stiffness, J, for different foundation soils, where ρ_c is rate of increase in undrained shear strength with depth (kPa/m) (modified from Rowe and Soderman 1987b): (a) $s_{uo} = 5$ kPa, (b) $s_{uo} = 10$ kPa, (c) $s_{uo} = 15$ kPa

allowable pressure in excess of a factor of 2 may be achieved with high-stiffness reinforcement. The potential for achieving these increases is also controlled by the strength of soil–reinforcement interface (the undrained shear strength of the foundation soil at the ground level). For example, a comparison of the results given in Figures 13a and 13c for $\rho_c = 2$ kPa/m, indicates that, for an interface strength of 15 kPa, the increase in allowable pressure with reinforcement stiffness is much greater than that for the case with an interface strength of 5 kPa. The effectiveness of reinforcement is also influenced by the stiffness of the foundation crust. For embankments on soft brittle soils with a high-strength crust, the effect of the crust dominates, even if a very high tensile stiffness geosynthetic is used (Mylleville and Rowe 1991).

The approach proposed by Rowe and Soderman (1985a) for embankments on soil whose strength is constant with depth limits the force in the geosynthetic corresponding to an allowable compatible strain, which was deduced from the analysis of unreinforced embankments. This approach worked well, since for these cases the reinforced collapse mechanism was similar to the unreinforced collapse mechanism. However, this is not the case when embankments are constructed on a foundation whose strength increases with depth. For these cases, the inclusion of reinforcement changes the strain pattern, giving rise to a much deeper collapse mechanism passing through stronger and stiffer soil (Figure 11). Thus the allowable 'compatible strain' which is deduced for the unreinforced case is not representative of the reinforcement strains developed prior to failure for reinforced embankments. The reinfor-

cement strain mobilized at the maximum net embankment height (i.e. onset of embankment failure) can be estimated from field instrumentation or finite element analysis. Hinchberger and Rowe (2003) found that strain at embankment failure was strongly influenced by the kinematics of the collapse mechanism developed within the foundation soil, the undrained shear strength at the ground surface, and the rate of increase in strength with depth. The reinforcement strain at failure can be estimated from Figure 14. However, the strain may be limited by the strain at rupture of the reinforcement. Also, for soft brittle foundation soils which are susceptible to strain-softening, the limiting reinforcement strain may be as low as 0.5–2% in order to reduce the maximum shear strain developed in the foundation soil to acceptable levels (Rowe and Mylleville 1990; Mylleville and Rowe 1991).

4.4. Multiple layers of reinforcement

Rowe and Mylleville (1990) found that the failure height of a reinforced embankment was essentially the same for two closely spaced layers of geosynthetic with a given tensile stiffness and a single layer with twice the stiffness. They also found that the maximum geosynthetic strains at failure were essentially the same for two layers as for one layer of reinforcement when the sum of stiffness was the same for the two-layer system as for the stiffness of the single-layer system.

4.5. Foundations with surface crust

Humphrey and Holtz (1989) showed that the effect of reinforcement on the embankment stability and deformations was dependent on the strength and compressibility of the surface crust of the soft foundation. The increase in embankment failure height due to the use of a given type of basal reinforcement increases as the crust strength decreases and compressibility increases. This is consistent with the finding by Rowe and Mylleville (1990) that, for a deposit with a crust, very high stiffness reinforcement may be required to mobilize significant force prior to embankment failure. For a surface crust with weak zones, reinforcement can be an effective means of increasing embankment stability (Humphrey and Holtz 1989).

5. PARTIALLY DRAINED BEHAVIOUR OF REINFORCED EMBANKMENTS

An examination of the construction-induced excess pore pressures observed in a large number of field cases suggests that significant partial consolidation of the foundation may occur during embankment construction at typical construction rates (Leroueil *et al.* 1978; Crooks *et al.* 1984; Leroueil and Rowe 2001). This applies to natural soft cohesive deposits that are typically slightly overconsolidated, and in a number of cases cited in Section 3 it has been reported that there was significant strength gain due to partial consolidation during embankment construction (e.g. Volk *et al.* 1994; Varuso *et al.* 1999; Lau and Cowland 2000). This issue requires more consideration than it has been given in the past, and is discussed in the following subsections.

5.1. Single-stage construction of reinforced embankments

Although field cases suggest the importance of considering partial drainage, they do not allow a direct comparison of cases where it is, or is not, considered. However, finite

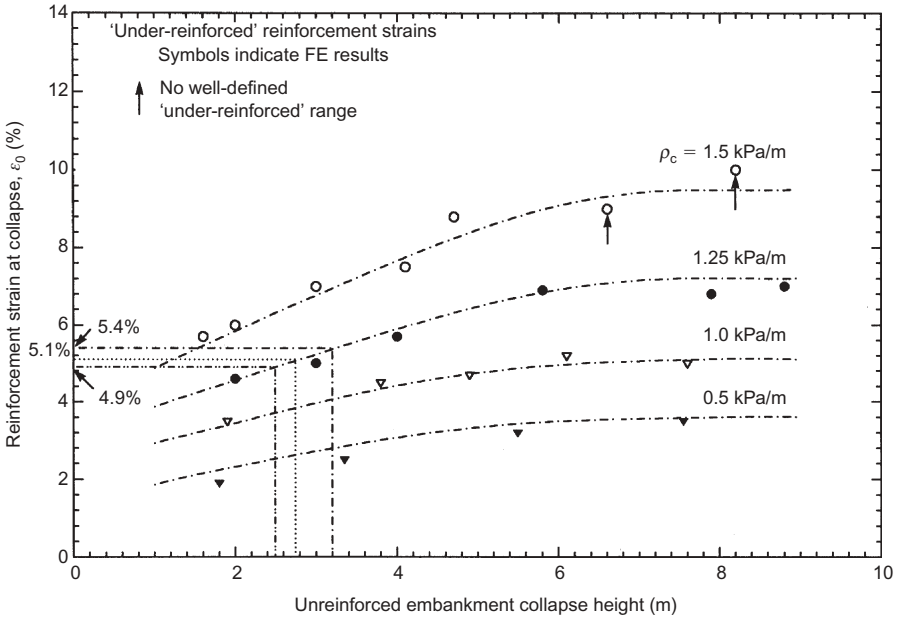

Figure 14. Chart for estimating reinforcement strains at embankment failure for foundation soils with strength increase with depth (modified from Hinchberger and Rowe 2003). (Note: This chart only considers soil–reinforcement interaction, and the allowable strain may be limited to a lower value by the allowable reinforcement strain based on the strain at rupture)

element analyses do provide a powerful tool for comparing the behaviour of reinforced embankments constructed under undrained and partially drained conditions (Rowe and Li 1999). For example, foundation soil A (Figure 15) gave rise to the calculated variation in embankment failure height with reinforcement stiffness given in Figure 16 for undrained and partially drained conditions. For the undrained cases, the unreinforced embankment failure height was 2.1 m. A change of reinforcement stiffness from 500 kN/m to 8000 kN/m resulted in an increase in failure height by between 0.68 m to 1.44 m relative to the unreinforced case. The effect of reinforcement on the embankment failure height was most significant when J was increased from 500 kN/m to 2000 kN/m.

Fully coupled analyses which allowed for the dissipation of excess pore pressure during construction at a rate of about 1 m/month gave an increase in the unreinforced embankment failure height of 2.44 m (Figure 16). A change of reinforcement stiffness from 500 kN/m to 8000 kN/m resulted in an additional increase in failure height by between 0.71 m and 2.36 m (relative to the unreinforced case). Thus the reinforcement had a greater effect for the partially drained cases than for undrained cases. Again, the increase in reinforcement stiffness had the most significant effect on the embankment failure height for stiffness values up to $J = 2000$ kN/m.

Figure 17 shows the maximum reinforcement strain developed at embankment failure for both undrained and partially drained conditions assuming that the reinforcement can sustain these strains without reinforcement failure. For the reinforced embankments, the failure strains $\varepsilon_f = 1.3–6.1\%$ for undrained conditions can be compared with $\varepsilon_f = 3.2–6.5\%$ for partially drained conditions. This arises because the stronger foundation soil results in some change in the failure mechanism, which, in turn, results in higher reinforcement strain at failure. It is also worth noting that the maximum value for reinforcement strain at failure occurs at very different reinforcement stiffness values (i.e. 500 kN/m for the undrained case and 2000 kN/m for the partially drained case).

5.2. Multi-stage construction of reinforced embankments

When a foundation soil does not initially have the strength to safely support a given embankment, stage construction

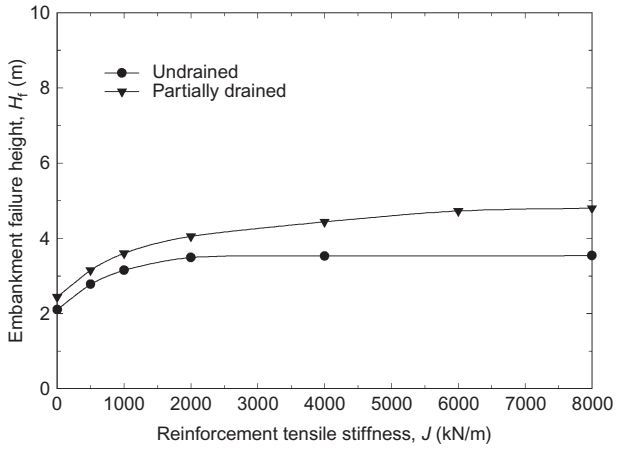

Figure 16. Embankment failure height against reinforcement tensile stiffness

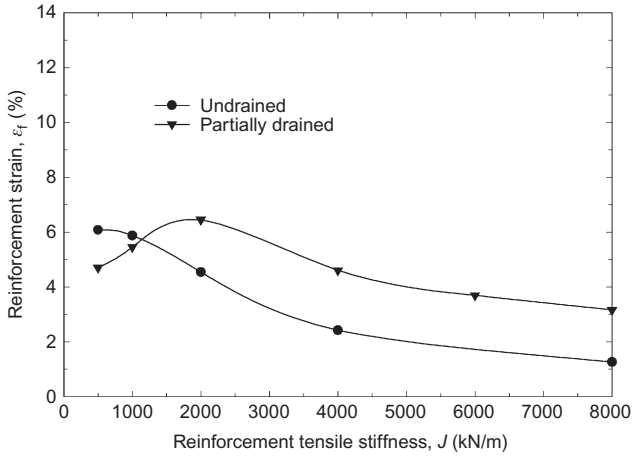

Figure 17. Reinforcement strain at failure (Soil profile A – Figure 15)

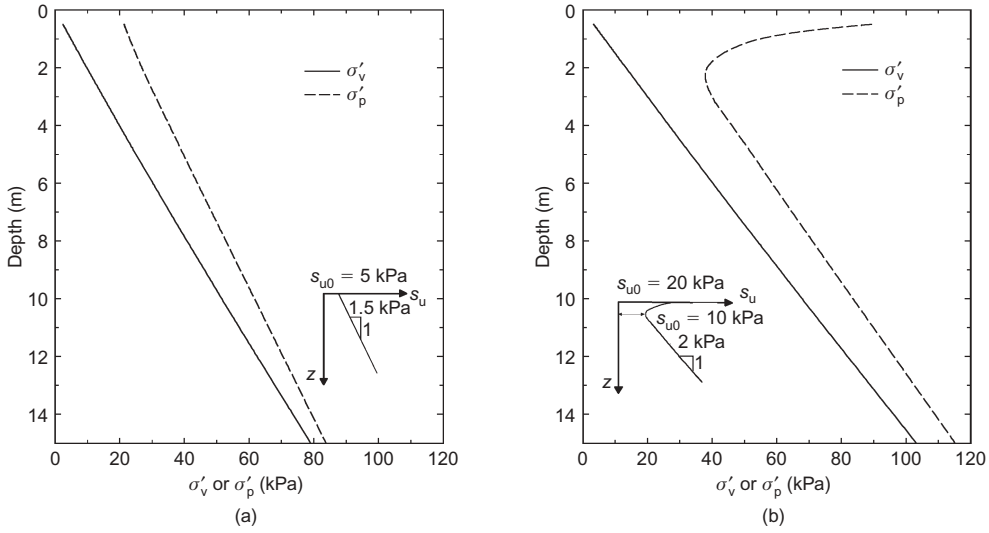

Figure 15. Preconsolidation profiles: (a) foundation soil A; (b) foundation soil B (after Rowe and Li 1999)

may be used to allow sufficient consolidation and strength gain to occur to support the final embankment load. Li and Rowe (1999a) showed that geosynthetic reinforcement may eliminate the need for stage construction or, in cases where staging was still needed, it reduced the number of stages required. For example (Figure 18), the failure height achieved with one-stage construction and reinforcement $J = 4000$ kN/m was similar to that obtained using reinforcement with $J = 2000$ kN/m and four-stage construction (with a 9-month consolidation period between stages and each embankment stage constructed to a height such that a factor of safety of 1.3 was maintained at the end of each stage except the last stage, which was constructed until the failure height was reached). The reason for the limited gain in failure height due to multi-stage construction is that, while there may be a significant dissipation of excess pore pressure during the early stages of loading (when the soil is initially overconsolidated), there is very little dissipation of excess pore pressure during the 9 months between construction stages once the soil becomes normally consolidated (because of the low hydraulic conductivity of the normally consolidated clay). In order to gain a greater improvement due to consolidation, one would either need a longer waiting period between construction stages or, alternatively, vertical drains could be used to speed up the dissipation of excess pore pressures.

In some cases the use of high-stiffness reinforcement may eliminate the need for stage construction and therefore shorten construction time.

The use of reinforcement enhances the benefit of partial consolidation of the foundation soil during single-stage construction (Figure 16). Reinforcement can also enhance the strength gain made in multi-stage construction (Figure 19). For example, results were obtained for embankments that were first constructed to the maximum height permitted with a factor of safety of 1.3 and then constructed to failure after an average of 95% consolidation of the foundation soil had been achieved at the end of stage one. The corresponding increases in failure height (relative to undrained conditions) achieved for different levels of reinforcement stiffness are shown in Figure 19. It

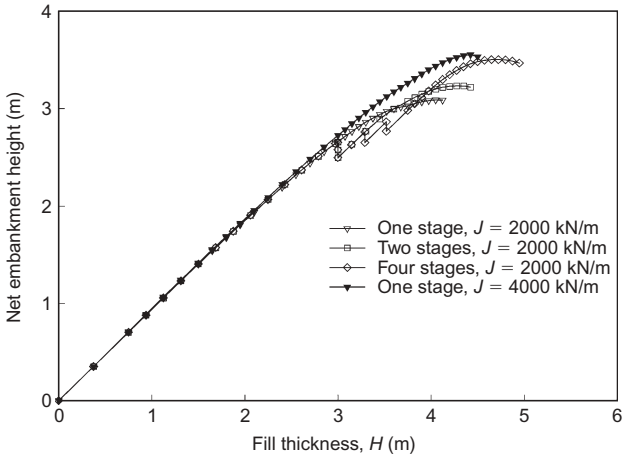

Figure 18. Effect of multi-stage construction on embankment height for Soil profile A

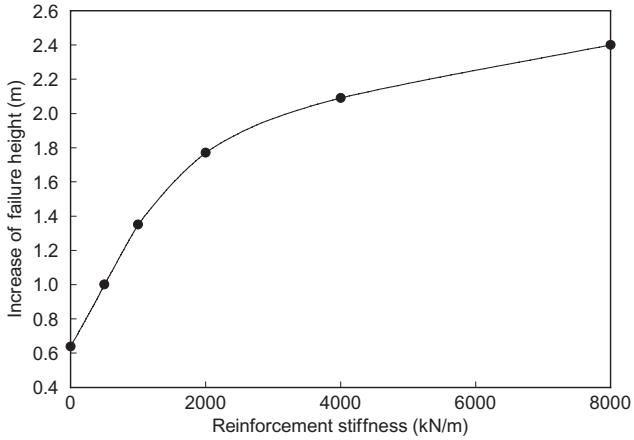

Figure 19. Increase of failure height after 95% consolidation at end of first stage of construction for Soil profile A

can be seen that the stiffer the reinforcement, the greater the increase in embankment failure height due to foundation soil strength gain. For example, the net increase in failure height was 0.6 m (from $H_f = 2.5$ m to $H_f = 3.1$ m) and 2.4 m (from $H_f = 4.8$ m to $H_f = 7.2$ m) for the unreinforced and heavily reinforced ($J = 8000$ kN/m) embankments respectively. This improvement occurs because the reinforcement helps to fully mobilize the shear strength of the foundation soil after consolidation. These results also imply that there may be benefit arising from combining reinforcement with methods of accelerating consolidation, such as PVDs, as discussed in the following section.

6. REINFORCED EMBANKMENTS WITH PVDs

6.1. Background

Since the first prototype of a prefabricated drain made of cardboard (Kjellman 1948), prefabricated vertical drains (also called wick drains) have been widely used in embankment construction projects (e.g. Hansbo *et al.* 1981; Nicholson and Jardine 1981; Jamiolkowski *et al.* 1983; Holtz 1987; Lockett and Mattox 1987; Holtz *et al.* 2001). Owing to the advantages of prefabricated vertical drains in terms of cost and ease of construction, PVDs have almost entirely replaced conventional sand drains as vertical drains. PVDs accelerate soil consolidation by shortening the drainage path and taking advantage of any naturally higher horizontal hydraulic conductivity of the foundation soil. This improves embankment stability owing to the strength gain in the foundation soil associated with the increase in effective stress due to consolidation.

The use of geosynthetic reinforcement in combination with prefabricated vertical drains has the potential to allow the cost-effective construction of substantially higher embankments in considerably shorter time periods than conventional construction methods (e.g. Lockett and Mattox 1987; Bassett and Yeo 1988; Schimelfenyg *et al.* 1990).

The synergistic effect of the combined use of reinforcement and prefabricated vertical drains has been investigated by Li and Rowe (1999b, 2001a). It has been shown that the use of PVDs in conjunction with typical construction rates results in relatively rapid dissipation of excess pore pressures. This can be enhanced by the use of geosynthetic reinforcement, as shown in the following sections.

6.2. The combined effect of reinforcement and PVDs

Figure 20 shows the variation of net embankment height with fill thickness from finite element simulations of reinforced embankment construction, where S is the spacing in a square pattern. For this particular foundation soil A (Figure 15) and PVDs at a spacing of 2 m, the unreinforced embankment can be constructed to a height of 2.85 m. If reinforcement with tensile stiffness $J =$ 250 kN/m is used, the failure height increases to 3.38 m. It is noted that, for the assumed soil properties and a construction rate of 2 m/month, the embankment will not fail owing to bearing capacity failure of the foundation soil if the reinforcement stiffness is greater than 500 kN/m. The findings from this finite element analysis are consistent with the findings of Sharma and Bolton (2001), who conducted centrifuge tests of reinforced embankments over foundations with PVDs and found that the PVDs in combination with basal reinforcement gave rise to better mobilization of tension in the reinforcement.

It is known that reinforcement can reduce the shear stress and consequent shear deformations in foundation soils. In fact both reinforcement and PVDs can decrease horizontal deformations in the foundation below the embankment toe (Figure 21). For a 3.5 m-high embankment over foundation soil profile A, the combination of PVDs and reinforcement with stiffness $J = 2000$ kN/m gave the least horizontal foundation displacement, while the case without PVDs and $J = 2000$ kN/m had the about the same horizontal displacements as the case with PVDs and $J = 1000$ kN/m. These findings are also consistent with the observations by Sharma and Bolton (2001) that the installation of vertical drains reduced the lateral spreading of the soft foundation based on centrifuge test results.

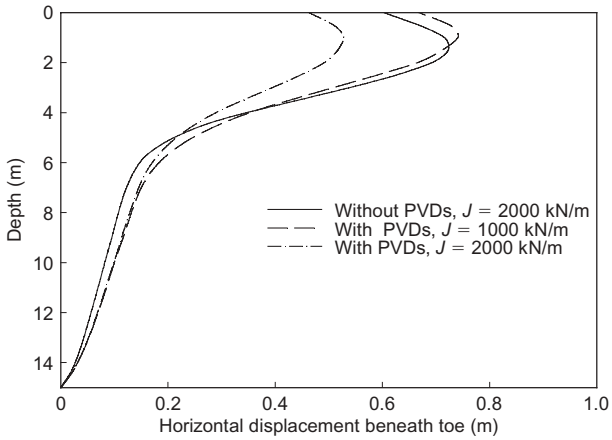

Figure 21. Comparison of horizontal displacements below toe at end of construction on Soil profile A, $H = 3.5$ m

6.3. The effect of construction rate

Owing to the drainage enhancement provided by PVDs, significant consolidation may occur during embankment construction. The partial consolidation that occurs during construction is a function of construction rate. Therefore construction rates may be an important factor influencing the stability of embankments.

Embankment stability is sensitive to construction rate, as is evident from the failure height shown in Figure 22 for an unreinforced embankment. It was found that there was a threshold construction rate below which the embankment would not fail owing to bearing capacity failure of the foundation soil. For the configuration of PVDs and two foundation soils examined, the threshold rate is 0.5 m/month and 2 m/month for soils A and B respectively. This implies that, if construction is controlled to a rate slower than this threshold rate, reinforcement is not needed to maintain embankment stability. Conversely, the use of reinforcement could efficiently increase embankment stability when the construction rate is greater than the threshold rate.

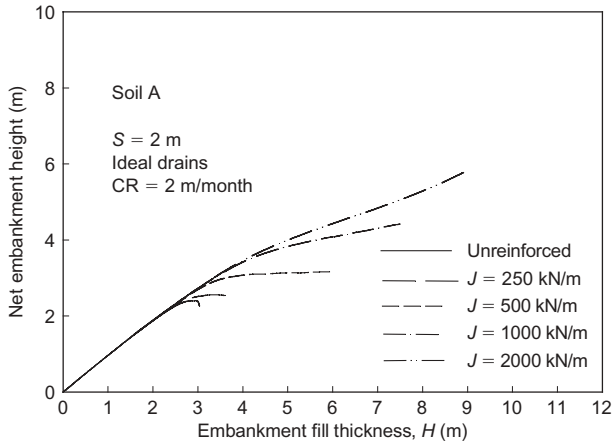

Figure 20. Variation of net embankment height with fill thickness

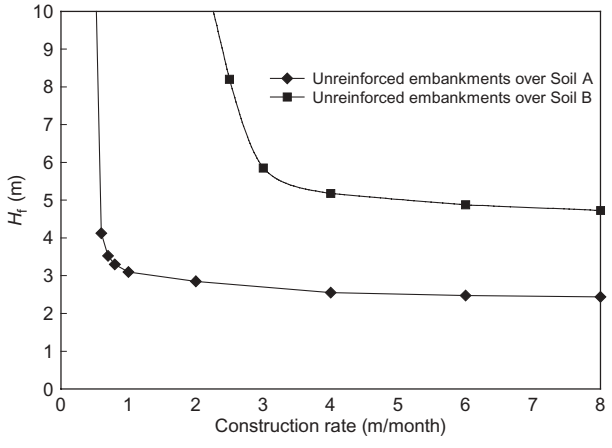

Figure 22. Effect of construction rate on embankment failure height, H_f (see Figure 15 for soil profiles)

6.4. Consolidation and strength gain due to PVDs

The use of PVDs to gain significant consolidation of foundation soils during construction has been reported in a number of cases cited in Section 3 (e.g. Lockett and Mattox 1987; Fritzinger 1990; Schimelfenyg *et al.* 1990; Volk *et al.* 1994). However, the magnitude and distribution of strength gain have received relatively little attention in the literature.

Based on finite element analyses, Li and Rowe (2001a) have shown that there is significant consolidation of foundation soils with PVDs. For example, Figure 23 shows the contours of the increase in undrained shear strength of the foundation soil during construction for two reinforced ($J = 2000$ kN/m) embankments having heights $H = 4.4$ m and 6.5 m over Soils A and B (Figure 15) respectively. For the sake of clarity, Figure 23 does not include the increase in undrained shear strength near the top and bottom layers, where the gradient of shear strength increase is high owing to the drainage boundary effects. Owing to the presence of the PVDs, the average increase in undrained shear strength was rather uniform throughout most of the thickness of the deposit (with some drainage boundary effects at the top and bottom of the foundation). The calculated increase in shear strength of soil under the embankment centre was 5 kPa (about 40% of the initial strength) for soil A and 11 kPa (about 50% of the initial strength) for soil B. The increase under the embankment slope was about 3 kPa (about 25% of the initial strength) for soil A and 6.5 kPa (about 30% of the initial strength) for soil B. It is evident that that the increase in shear strength during embankment construction is significant below the embankment, but it is also clear that the distribution of the change in undrained shear strength with position needs to be considered in assessing stability, since the geometry of critical failure mechanisms may change as a result of the change in magnitude and distribution of shear strength.

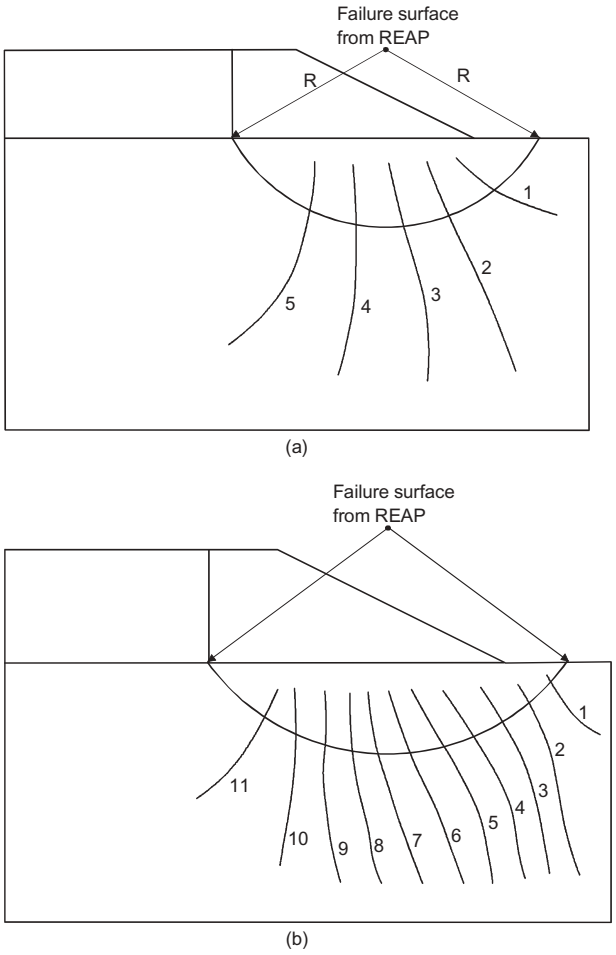

Figure 23. Contours showing increase in undrained shear strength, Δs_u in kPa, at end of construction, from FEM analyses: (a) Soil A, ideal drains, $S = 2$ m, $H = 4.41$ m, CR = 2 m/month; $J = 2000$ kN/m; (b) Soil B, ideal drains, $S = 2$ m, $H = 6.48$ m, CR = 4 m/month; $J = 2000$ kN/m; (after Li and Rowe 2001a)

In analyzing the consolidation of PVD-enhanced foundation soils during embankment construction, consideration should be given to radial and vertical drainage, construction rate, and the difference between consolidation coefficients of soils in the overconsolidated and normally consolidated stress ranges. Generally, a numerical analysis is needed to consider these factors. Li and Rowe (2001a) proposed an approximate method to calculate the consolidation of foundation soils allowing for the aforementioned factors. This method can be performed by hand, or by using a spreadsheet calculation, without numerical analysis as outlined below.

The analysis is greatly simplified by the fact that with PVDs the dissipation of pore pressures is essentially uniform with depth (except at the top and bottom boundaries), as implied by the strength gain contours shown in Figure 23. All assumptions of Terzaghi's consolidation theory are preserved except for the change in compressibility as a soil moves from the overconsolidated to normally consolidated state, the time-dependent loading and the presence of radial drainage paths. It is assumed that the soil becomes normally consolidated when the average degree of consolidation at a particular time is such that the average vertical effective stress of soils is equal to the preconsolidation pressure. At this time, the change of soil compressibility is a step change (i.e. from recompression index C_r to compression index C_c). The time-dependent loading is taken to be a linear ramp loading 0–A as shown in Figure 24. An embankment is constructed to apply a vertical stress of $\Delta\sigma$ over a period of time t_C. During the period to $t_{O/C}$, when the soil is overconsolidated, the consolidation is governed by the consolidation coefficient $C_{O/C}$, and after $t_{O/C}$ when the soil becomes normally consolidated, the consolidation is governed by consolidation coefficient $C_{N/C}$. For a deposit with two-way drainage, the average degree of consolidation at any time is defined as

$$\overline{U} = \frac{D\Delta\sigma(t) - \int_0^D u\,\mathrm{d}z}{D\Delta\sigma} \tag{17}$$

where D = the thickness of the deposit; $\Delta\sigma(t)$ = applied stress at time t; and u = excess pore pressure at time t. At time $t_{O/C}$ the applied stress $\Delta\sigma$(t) is $\Delta\sigma\ t_{O/C}/t_C$, the

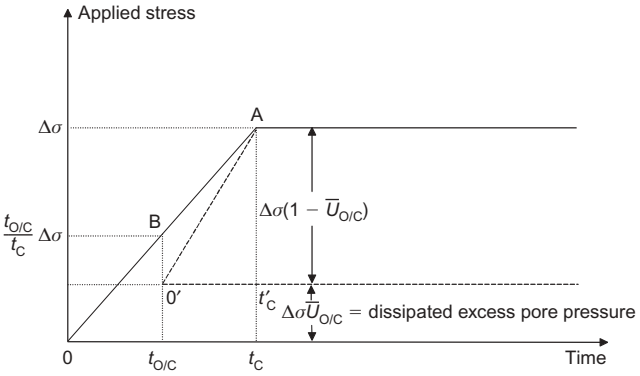

Figure 24. Breakdown of linear ramp load function for consolidation analysis considering the soil in its overconsolidated and normally consolidated states (modified from Li and Rowe 2001a)

average degree of consolidation is $\bar{U}_{O/C}$, and the average change in effective stress at this time is $\Delta\sigma\,\bar{U}_{O/C}$. The average excess pore pressure that needs to dissipate after application of the full stress $\Delta\sigma$ is $\Delta\sigma(1 - \bar{U}_{O/C})$, and it is assumed that this excess pore pressure is developed over a period of time $t'_C = t_C - t_{O/C}$. After $t_{O/C}$ the average degree of consolidation, $\bar{U}_{N/C}$, is calculated using $C_{N/C}$ for the ramp load of $\Delta\sigma(1 - \bar{U}_{O/C})$. Figure 24 shows that the linear load function O–A is replaced by two linear load functions: O–B and O′-A for soil in overconsolidated and normally consolidated states respectively. It is assumed that the average degree of consolidation under the load O–A after $t_{O/C}$ is equivalent to the average degree of consolidation under the load O′–A plus the average degree of consolidation under the load O–B that has occurred at time $t_{O/C}$. Thus, the total average degree of consolation at time $t \geqslant t_{O/C}$ is

$$\bar{U} = \bar{U}_{O/C} + \left(1 - \bar{U}_{O/C}\right)\bar{U}_{N/C} \tag{18}$$

To consider the consolidation of soil under a time-dependent loading, Olson (1977) derived relatively simple solutions considering both vertical and radial drainage for a linear ramp loading problem based on the assumptions of the classic consolidation theories except for the time-dependent loading. $\bar{U}_{O/C}$ and $\bar{U}_{N/C}$ can be calculated separately using Olson's (1977) solution as follows.

For vertical consolidation:

$$T \leqslant T_c\text{: } \bar{U}_v = \frac{T}{T_c}\left\{1 - \frac{2}{T}\sum\frac{1}{M^4}\left[1 - \exp\left(-M^2T\right)\right]\right\} \tag{19a}$$

$$T \geqslant T_c\text{: } \bar{U}_v = 1 - \frac{2}{T_c}\sum\frac{1}{M^4}\left[\exp\left(M^2T_c\right) - 1\right]\exp\left(-M^2T\right) \tag{19b}$$

where T is the time factor for vertical consolidation; T_c is the time factor at the end of construction; and $M = \pi(2m + 1)/2$, $m = 0, 1, 2, 3,\ldots$ until the sum of all remaining terms is insignificant.

For horizontal (radial) consolidation:

$$T_h \leqslant T_{hc}\text{: } \bar{U}_h = \frac{1}{T_{hc}}\left\{T_h - \frac{1}{A}\left[1 - \exp\left(-AT_h\right)\right]\right\} \tag{19c}$$

$$T_h \geqslant T_{hc}\text{: } \bar{U}_h = 1 - \frac{1}{AT_{hc}}\left[\exp\left(AT_{hc} - 1\right)\right]\exp\left(-AT_h\right) \tag{19d}$$

where T_h is the time factor for horizontal consolidation; T_{hc} is the time factor at the end of construction; and $A = 8/\mu$ (μ is defined in Section 4) using Hansbo's solution for vertical drains.

Combined vertical and radial consolidation using the method of Carrillo (1942):

$$\bar{U} = 1 - (1 - \bar{U}_h)(1 - \bar{U}_v) \tag{19e}$$

Li and Rowe (2001a) verified this approximate method by comparing results using this approach to calculate $\bar{U}$ with values obtained from finite element analyses, and showed that this method (Figure 24) significantly improved the accuracy compared with traditional methods.

As shown in Figure 23, the variation of the strength gain with depth is relatively uniform for a relatively uniform foundation soil, and the magnitude of strength gain for soil along the failure surface gradually decreases from a maximum below the embankment crest to a minimum in front of the embankment toe. Based on the average degree of consolidation of the foundation soil (i.e. Equation 17), the strength gain of soils beneath the embankment centre can be estimated as follows using the SHANSEP method (Ladd and Foott 1974) assuming that the embankment loading is one-dimensional:

$$\Delta s_{uc} = \left[\alpha\left(\sigma'_{vo} + H\gamma_{fill}\,\bar{U}\right)\right] - s_{uo} \tag{20}$$

where the ratio $\alpha = s_u/\sigma'_p$ is constant for a given soil, and σ'_{vo} and s_{uo} are the initial vertical effective stress and undrained shear strength prior to embankment construction respectively.

For the locations along the potential slip surface below the embankment slope, the strength gain can be estimated using the method proposed by Li and Rowe (2001a) as follows:

$$\Delta s_{uf} = \left[\beta\left(\sigma'_{mi} + \gamma_{fill}HI_q\,\bar{U}_f\right)\right] - s_{uo} \tag{21}$$

where

$$\beta = \frac{3}{1 + 2K'_0}\alpha \tag{22}$$

and σ'_{mi} is the initial effective mean stress; I_q is the influence factor for total mean stress σ_m based on elastic solutions (e.g. Poulos and Davis 1974); $\bar{U}_f$ is the average degree of consolidation of soils along the potential failure surface (i.e. with respect to applied stress of $\Delta\sigma_m = \gamma_{fill}HI_q$); and K'_0 is the coefficient of lateral earth pressure at rest for soil in its normally consolidated state. The methods for the estimation of strength gain described herein can be used in the design of the combined use of reinforcement and PVDs, as shown in the following section.

6.5. Design of reinforcement and PVDs

Design of the reinforced embankment and PVDs are usually treated separately in current design methods even if both reinforcement and PVDs are used together. The design of reinforced embankments is usually based on undrained stability analyses without consideration given to the effects of PVDs (e.g. Jewell 1982; Mylleville and Rowe 1988; Holtz *et al.* 1997). On the other hand, the design of PVDs is based on consolidation analyses, and the drain spacing is selected to achieve a required degree of consolidation within an allowable time period (e.g. Holtz *et al.* 1991, 2001).

Li and Rowe (2001a) proposed a design method allowing for the combined effects of reinforcement and prefabricated vertical drains. Within a limit state design philosophy, this method uses an undrained strength analysis (USA) method suggested by Ladd (1991) with a total stress analysis allowing for strength gain of a foundation soil at the time to be considered. The approach is summarized as follows.

(1) Select design criteria:
- H, B, n — height, width and slope of embankment;
- $\overline{U}$ — average degree of consolidation required;
- t — available time to achieve $\overline{U}$;
- CR — construction rate.

(2) Select soil parameters for the embankment fill and foundation:
- s_u — undrained shear strength profile;
- σ'_p, σ'_v — preconsolidation pressure and current vertical effective stress with depth;
- K'_0 — coefficient of lateral earth pressure at rest profile;
- s_u/σ'_m — Normalized shear strength for soil in its normally consolidated state, where σ'_m = effective mean stress $= (1 + 2K_0)\sigma'_v/3$ for soil in its normally consolidated state;
- $C_{O/C}$, $C_{N/C}$ — coefficient of consolidation of soil in overconsolidated and normally consolidated states;
- k_h, k_v — horizontal direction and vertical hydraulic conductivity for undisturbed soil;
- k_s — hydraulic conductivity of disturbed soil;
- H_d — length of longest drainage path in vertical direction;
- ϕ, γ_{fill} — friction angle and unit weight of embankment fill.

(3) Select a prefabricated vertical drain system:
- S — spacing of PVDs (determined during design iterations);
- D_e — effective diameter of drain influence zone, $= 1.05S$ for triangular pattern, $1.13S$ for square pattern;
- L — length of single drain (equal to the thickness of clayey deposits in most cases);
- d_s — diameter of smear zone caused by drain installation;
- d_w, q_w — equivalent diameter and discharge capacity of single drain.

(4) Calculate the average degree of consolidation at the available time, t, using Equations 17–18. If the calculated average degree of consolidation is less than required $\overline{U}$, repeat Step 3 to select a new PVD configuration (e.g. spacing, S, and length, L) until $\overline{U}$ is met.

(5) Estimate the average influence factor I_q ($\Delta\sigma_m = \gamma_{fill} H I_q$) for the increase in total mean stress of the foundation soil along the potential slip surface using elastic solutions (e.g. Poulos and Davis 1974; Li and Rowe 2001a).

$$\Delta\sigma_m = \tfrac{1}{3}(\Delta\sigma_x + \Delta\sigma_y + \Delta\sigma_z) \tag{23}$$

$$I_q = \frac{\Delta\sigma_m}{\Delta\sigma} \tag{24}$$

(6) Calculate the average degree of consolidation along the potential slip surface at the end of the embankment construction, $\overline{U}_f$.

(7) Estimate the average strength increase, Δs_{uf}, of soil along the potential failure surface at the end of construction using Equation 21.

(8) Factor strength of soils using partial factor f_c for undrained shear strength of foundation soil ($s^*_u = s_u/f_c$) and f_ϕ for fill material ($\tan\phi'^* = (\tan\phi')/f_\phi$), and f_γ for unit weight of fill γ_{fill} ($\gamma^*_{fill} = \gamma_{fill} f_\gamma$) as appropriate.

(9) Factor Δs_{uf} using partial factor f_c ($\Delta s^*_{uf} = \Delta s_{uf}/f_c$).

(10) Using a limit equilibrium method calculate the equilibrium ratio (ERAT) of restoring moment to overturning moment for the embankment without reinforcement using the factored soil parameters of embankment fill and factored undrained shear strength profile including the strength gain during construction, i.e. ($s^*_u + \Delta s^*_{uf}$). If ERAT $\geqslant$ 1.0, reinforcement is not needed. If ERAT $<$ 1.0, reinforcement is needed; continue with the following steps.

(11) Use a limit equilibrium program designed for the analysis of reinforced embankments (e.g. REAP: Mylleville and Rowe 1988) to calculate the required reinforcement tensile force, T_{req}, using new factored undrained shear strength profile obtained in step 10 (T_{req} is the force required to give overturning moment = restoring moment based on factored soil properties, i.e. ERAT = 1).

(12) Choose an allowable strain, ε_{all}, for the reinforcement. Then the required reinforcement tensile stiffness is calculated as follows:

$$J_{reg} = \frac{T_{req}}{\varepsilon_{all}} \tag{25}$$

In this procedure, the limit states examined involve failure of the embankment, the foundation, and failure of reinforcement. All calculations except the slope stability analysis can be done by hand or using a spreadsheet program. This approach can be made equally applicable to a stage construction sequence by adding the consolidation

during stoppage in step 4 and 6 while keeping other steps the same. Design parameters (e.g. S, L, T_{req} and J_{req}) can be obtained iteratively from steps 1 to 12. In the design iteration, the construction rate and stage sequences can be varied such that the design grade can be achieved in an optimum time schedule. In order to ensure embankment stability during construction, it is essential to monitor the development of reinforcement strains, excess pore pressures, settlement and horizontal deformations, and to confirm that observed behaviour is consistence with the design assumptions. A worked example of the use of this design method has been given by Li and Rowe (2001a).

7. REINFORCED EMBANKMENTS OVER PEAT

7.1. Background

As discussed in Section 3.7, fibrous peats are characterized by high water content, void ratio, hydraulic conductivity and compressibility. However, organic soils can vary substantially in terms of their engineering properties and response to embankment loads. There are many different classification systems (Landva *et al.* 1983) for peat, which may have a highly variable inorganic component (ranging from less than 20% to 80% ash content). Thus the term 'peat' is often used to include a vast range of organic soils, which may range from jelly-like organic silts and very soft organic clay muds to extremely coarse meshes of wood remains and fibres. Peat with 80% ash content and a significant clay component will respond to embankment loads in a manner similar to a clay, whereas a fibrous peat with less than 20% ash content may behave more like a frictional material than a cohesive material. For the purpose of this paper, the term 'peat' is reserved for soils with less than 20% ash content.

Owing to the high void ratio and compressibility of peats, it is usually not practical to obtain realistic strength parameters from conventional triaxial tests owing to excessive deformation rather than shear failure under compression (Adams 1961; Edil and Dhowian 1981; Rowe *et al.* 1984b). Also, it may be difficult to obtain reliable strength parameters from direct shear tests for some peats owing to their fibrosity. Landva (1980) has had success using the ring shear apparatus. Rowe (Rowe *et al.* 1984b; Rowe and Mylleville 1996; and various unpublished reports) has had considerable success with the Norwegian simple shear apparatus. which gave measured friction angles typically between 26° and 29° for a number of peats.

The failures of peat foundations do not usually involve the formation of a definite sliding surface or bearing capacity failure (e.g. Ripley and Leonoff 1961; Lupien *et al.* 1983). This is due to the fact that peats can experience significant dissipation of pore pressures during embankment construction at typical construction rates. Therefore, in the analysis of embankment performance, the use of effective deformation and strength parameters (combined with pore pressures) provided the best agreement between calculated and observed behaviour (Rowe *et al.* 1984a, 1984b).

The basal reinforcement can contribute to increasing the embankment stability as shown in Figure 25, where a reinforced embankment on a peat layer is underlain by very soft clay. The active earth pressure in the fill creates a lateral thrust. The applied pressure due to the embankment resting on the peat also induces a lateral thrust. Generally, owing to the low effective stress in the peat outside the embankment, the passive resistance is negligible. Thus, the reinforcement and the shear strength at the peat/soft clay interface must resist the lateral force.

7.2. Rate of loading

Since the initial effective stress both within the peat and in any very soft clay or silt layer below the peat is very low, it is critical to monitor excess pore pressures and control the construction rate in order to increase the effective stress and shear resistance of the peat and soils. Even with very high-strength reinforcement there is a limit to the embankment height that can be achieved in single-stage construction owing to the low shear strength of the peat and the underlying soft soil. Therefore, stage construction and/or a controlled construction rate is recommended for embankments over peat foundations.

Weber (1969) reported that, in his experience with peat deposits in the San Francisco Bay area, fills in excess of 1.5 m above original ground level were subject to collapse. The exact height at which instability occurred depended

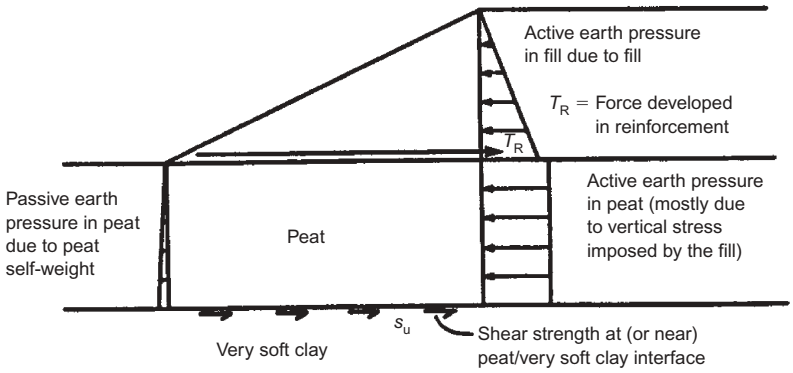

Figure 25. Potential failure mechanism due to lateral thrust and sliding on a deeper low-strength layer (e.g. very soft clay beneath a peat layer)

upon the foundation condition and rate of loading. At a construction rate of 0.9 m of fill per week he reported a collapse of a fill at a height of 2.4 m. At an even slower construction rate (0.15–0.3 m per week) fills to a height of about 3 m could be constructed without failure.

Both field and laboratory observations have indicated that embankments constructed on peat settle rapidly during construction and then continue to settle at a reduced rate after construction (e.g. Adams 1961; Weber 1969; Rowe *et al.* 1984a). An examination of the time–settlement curves indicates that primary consolidation occurs relatively quickly (typically 5–200 days after construction) even though 'creep-induced pore pressures' may remain for considerable periods during secondary compression.

Based on data in the literature, it appears that, where drainage of the peat is provided and a slow rate of construction is used, there will be little difficulty in constructing low (2 m or less) embankments on peat, although settlements may be large. However, when an impervious fill is used, or where the peat is underlain by soft marl or clay, it may not be possible to construct even low embankments on the peat unless special measures are taken to ensure stability (e.g. provide drainage, berms, geosynthetic reinforcement or use lightweight fill).

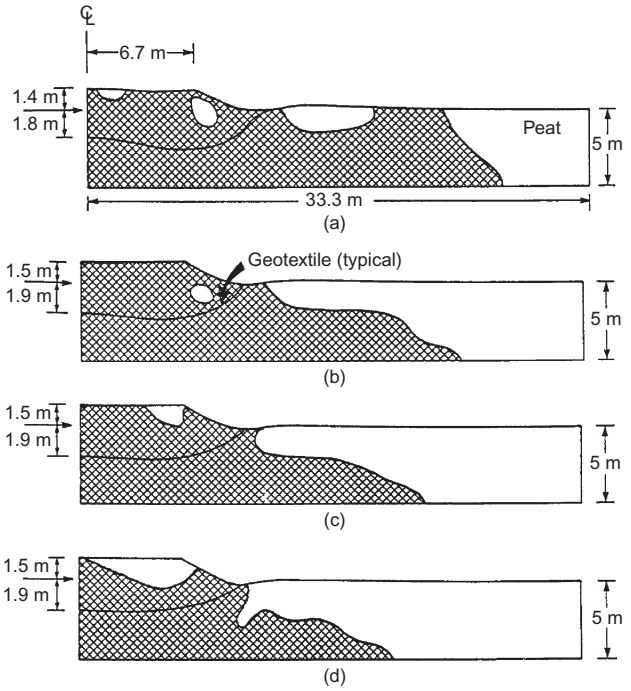

Figure 26. Deformed profile and plastic regions for embankment approximately 1.5 m above original ground level at end of construction, $B_{max} = 0.34$: (a) no reinforcement; (b) $J = 150$ kN/m; (c) $J = 500$ kN/m; (d) $J = 2000$ kN/m (after Rowe and Soderman 1985b)

7.3. Embankments on peat underlain by a firm base

Embankments constructed on peat underlain by a firm foundation are less prone to collapse, although some cases have been reported. For example, Ripley and Leonoff (1961), Flaate and Rygg (1964) and Lupien *et al.* (1983) reported 'shear failures' which, on the basis of the published data, do not appear to involve failure in the soil underlying the peat. These failures do not usually involve the formation of a definite sliding surface. Rather, the collapse involves rapid and excessive shear deformations, which give rise to large embankment settlement, lateral movement and mud waves.

Rowe and Soderman (1985b) have reported the results of a series of analyses which were performed to examine the effect of geosynthetic reinforcement on the stability and deformation of embankments on peat. The effect of geosynthetic reinforcement is illustrated in Figure 26. The cases examined involved granular fill ($c' = 0$, $\phi' = 32°$ and $\gamma = 21$ kN/m) and peat (with typical parameters: $c' = 1.8$ kPa, $\phi' = 27°$, $K_0' = 0.19$ and $e_o = 9$) and a construction rate limited to ensure that the excess pore pressure at the end of construction gave $B_{max} = 0.34$. Figure 26a shows the plastic region obtained in attempting to construct the embankment to 1.5 m without reinforcement. The fact that the geosynthetic reinforcement may improve the performance of the embankment can be appreciated by comparing the size of the plastic regions and the deformations of the original ground surface line beneath the shoulder of the embankment in Figures 26b, 26c and 26d with that in Figure 26a. The unreinforced embankment has the most settlement beneath the shoulder caused by the rotational movement of the embankment slope. A geosynthetic with a tensile stiffness, J, of 2000 kN/m gives a far more satisfactory dish-shaped settlement profile, as shown in Figure 26d.

7.4. Embankments on peat underlain by soft sediments

Peat deposits are typically encountered in regions which have been subjected to recent glaciation. Frequently, the depositional history of these deposits involves the sedimentation of clay, silts or lake marl (which may have some organic content) followed by the formation of a peat deposit. Because the peat has low unit weight, the clay, silt or marl in a recent normally consolidated deposit will be very weak just below the peat. Under embankment loadings, the underlying soft sediments will behave in an undrained manner. For the cases reported in the literature, the vane shear strength in a very soft stratum below the peat is typically in the range from 5 to 15 kPa, although shear strengths as low as 2.5–3 kPa have been reported (e.g. Lea and Brawner 1963). It has been reported that construction and maintenance problems and shear failure are far more likely to occur when the peat is underlain by a weak soil than when it rests on a firm stratum (e.g. Lea and Brawner 1963; Raymond 1969).

7.5. Design considerations based on finite element results

Rowe and Soderman (1985b, 1986) have conducted extensive finite element analyses of reinforced embankments on peat underlain by firm or soft deposits. The results have provided a means for design of reinforced embankments on such foundations. For the case of a firm

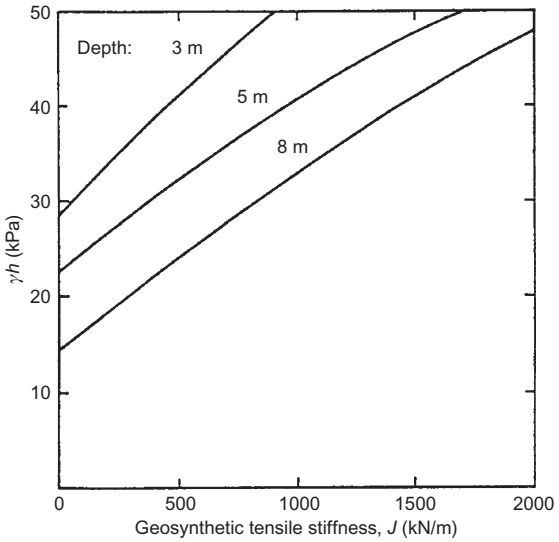

Figure 27. Design chart for peat underlain by a firm base: $\bar{B}_{max} = 0.34$; h = height of embankment above original ground level; γ = unit weight of fill (after Rowe and Soderman 1985b)

base, the expected variation in required tensile stiffness with design height is shown in Figure 27. The geosynthetic to be used should have a secant tensile stiffness (over the strain range from zero to the expected strain) greater than or equal to that taken from the chart. Table 2 summarizes the cases where the analyses indicated that an embankment could be constructed to a particular height, h, of 1, 1.5, 2 or 2.5 m above the original ground level assuming a value of B_{max} in the peat equal to 0.34 and other parameters as given by Rowe and Soderman (1985b, 1986). Note that the fill thickness, H, will be considerably greater than the height, h, above original grade owing to settlement that occurs during construction (i.e. $H = h +$ EOC settlement). The height, h, should include any surcharge that may be applied prior to pore pressure dissipation.

The tensile stiffness of the geosynthetic required to provide stability under the assumed conditions together with the expected maximum geosynthetic strain under these conditions is given in Table 2. For a number of cases, a range of tensile stiffness values is given. The analysis would indicate that the embankment could be constructed using a geosynthetic with a tensile stiffness within the range specified. However, if the conditions are as bad as assumed, the embankment would be very close to failure using geosynthetics at the low end of the stiffness range, and for these cases it would be far better to adopt a geosynthetic with a tensile stiffness in the upper end of the specified range. If there is a competent root mat and/or the anticipated value of B_{max} is less than 0.25, then a geosynthetic with a tensile stiffness in the lower end of the range may be adequate.

The numbers given in brackets in Table 2 represent the expected maximum strain in the given geosynthetic for the worst assumed conditions. The expected force in the geosynthetic can be deduced from the strain and the tensile stiffness. Since the strains are sensitive to construction sequence, strains greater than or less than those indicated in Table 2 may be anticipated under some circumstances, and any geosynthetic selected should have an adequate factor of safety against failure of the geosynthetic itself. Thus a geosynthetic should be selected which (a) has an appropriate tensile stiffness, and (b) has an adequate factor of safety against failure of the geosynthetic.

8. REINFORCED EMBANKMENTS OVER RATE-SENSITIVE SOILS

Natural soft cohesive deposits often exhibit viscous behaviour, and hence the undrained shear strength is strain-rate dependent (Casagrande and Wilson 1951; Graham *et al.* 1983; Leroueil and Marques 1996). Graham *et al.* (1983)

Table 2. Reinforced geosynthetic tensile stiffness values for embankments on fibrous peat (for limitations, see Rowe and Soderman 1986)

Peat thickness (m)	Underlying strata	Strength of underlying strata (kPa)	Maximum height, h, of fill above original ground level (m)			
			1	1.5	2	2.5
3	Firm	–	NRR[a]	NRR	500 (5%)	1000 (6%)
	2 m clay	15	NRR	NRR	500 (5%)	1000 (6%)
		10	NRR	NRR	500 (6%)	1000 (6.5%)
		7.5	NRR	150 (10%)	500 (8%)	1000 (7%)
		5	NRR	150 (14%) – 500 (8%)	2000 (4%)	PF
		2.5–5	150[b] (10%)[c]	2000 (5.5%)	PF[d]	PF
5	Firm	–	NRR	150 (14%) – 500 (6.5%)	500 (9.5%) – 1000 (5.5%)	1000 (6.5%) – 2000 (4%)
	3 m clay	15	NRR	150 (14%) – 500 (6.5%)	500 (9.5%) – 1000 (5.5%)	1000 (6.5%) – 2000 (4%)
		10	150 (5%)	500 (8.5%) – 1000 (7.5%)	2000 (5.5%)	PF
		7.5	500 (5%)	1000 (8.5%) – 2000 (5%)	PF	PF
8	Firm	–	350 (15%) – 1000 (7%)	500 (14%) – 1000 (8%)	1000 (9%) –2000 (6%)	2000 (6%)

[a]NRR = No reinforcement required.
[b]Minimum tensile stiffness value.
[c]Expected reinforcement strain for geosynthetic with the tensile stiffness indicated.
[d]PF = Reinforcement alone is not sufficient to provide stability, and failure is expected for these conditions unless additional measures are taken to ensure stability.

observed that, for a number of cohesive soils, an order of magnitude increase in the strain rate during laboratory shear typically resulted in increase of the measure undrained shear strength by between 10% and 20%. Kulhawy and Mayne (1990) compiled data obtained from 26 different rate-sensitive clays and showed that an average increase in undrained shear strength typically equaled 10% per logarithm cycle of strain rate (Figure 28).

8.1. Critical stage and critical strain rate

Owing to the viscoplastic behaviour of foundation soils, embankments may experience significant post-construction creep deformations or even failure some time after construction when the excess pore pressures increase or remain at a nearly constant level following the completion of construction (Crooks *et al.* 1984; Kabbaj *et al.* 1988; Keenan *et al.* 1986; Rowe *et al.* 1996). Under embankment loading, the excess pore pressure and deformation response of rate-sensitive foundation soft soils are often reported to be anomalous compared with the response described or predicted by the classical consolidation theory. For example, Rowe *et al.* (1996) showed that at the Sackville test site substantial vertical and horizontal displacements were recorded in the absence of pore pressure dissipation during periods of a constant embankment load. Kabbaj *et al.* (1988) summarized a number of embankment cases where the excess pore pressure increased to a maximum value at times after the end of construction ranging from a few days to as much as 150 days after the construction. Crooks *et al.* (1984) reported that, for 11 of the 31 cases they examined, the excess pore pressure in the foundation soils continued to increase significantly following completion of loading, and at six sites very slow or insignificant porewater pressure dissipation occurred for long periods following construction. These field observations have indicated that the immediate end of construction is not necessarily the most critical stage for embankments on rate-sensitive foundation soils.

Duncan and Schaefer (1988) found that at a constant embankment height the force in the reinforcement increased with time owing to undrained creep in the foundation soil.

This section presents some results from finite element analyses of a reinforced embankment over a rate-sensitive foundation, denoted as Soil C-R1, which was modeled using the Elliptical Cap viscoplastic constitutive relation (Rowe and Hinchberger 1998). This rate-sensitive soil has properties similar to Sackville soil described by Rowe and Hinchberger (1998). The liquid limit, plasticity index and natural water content of Soil C-R1 were approximately 50%, 18% and 53% respectively, and the undrained shear strength increases by about 16% per logarithm cycle of strain rate (Figure 28). The limit equilibrium analysis based on the undrained strength at a strain rate of 4.8% per hour (recommended by Bishop and Henkel 1962 for triaxial compression tests) indicates that the design height of 6.75 m can be achieved using a reinforcement with design stiffness $J = 2000$ kN/m and ultimate strength of 200 kN/m at 10% strain.

Figure 29 shows the development of maximum reinforcement strains for a 6.75 m-high reinforced embankment on this rate-sensitive soil. The maximum reinforcement strain of 5.8% at the end of construction (EOC) exceeded the design limit of 5% based on limit equilibrium analysis. Furthermore, it kept increasing after the end of construction and reached the failure strain of 10% at 163 h (6.8 days) after the end of construction. The breakage of

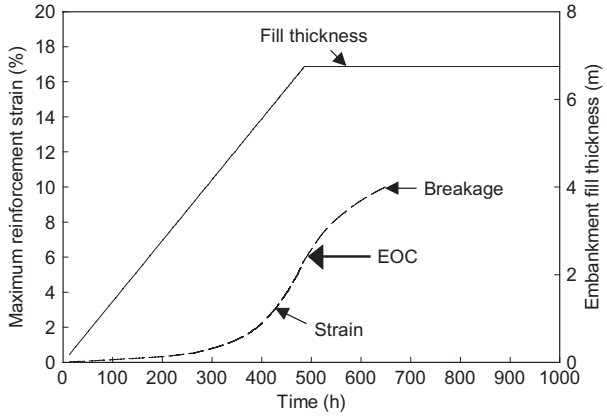

Figure 29. Reinforcement strain developed during short-term for embankments with CR = 10 m/month, $J = 2000$ kN/m over Soil C-R1

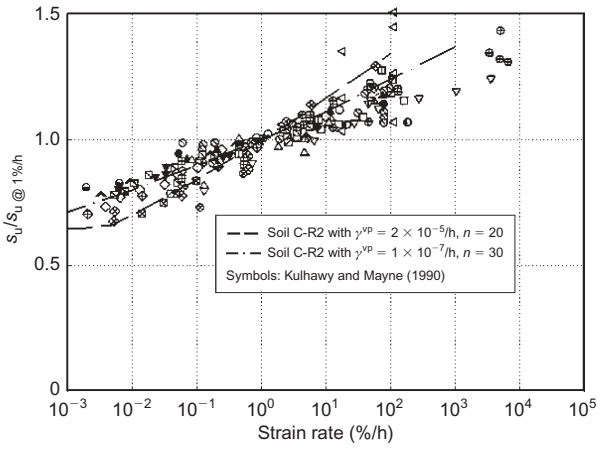

Figure 28. Effect of strain rate on undrained shear strength s_u of Soils C-R1 and C-R2 (after Li and Rowe 2002)

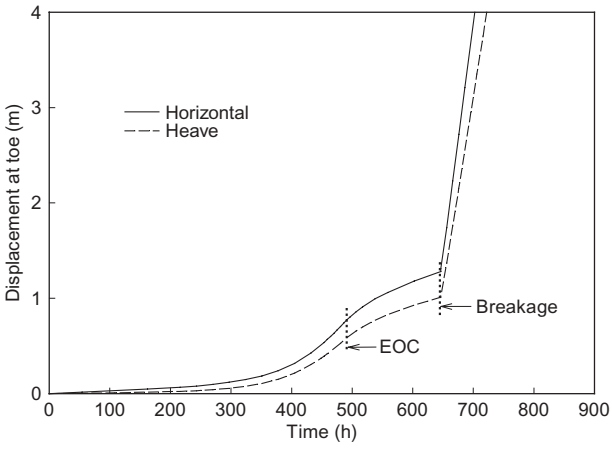

Figure 30. Displacements at toe for case with $J = 2000$ kN/m, $H = 6.75$ m and reinforcement breaking at $\varepsilon = 10\%$

reinforcement can result in the failure of the embankment, as was the case in the test embankment reported by Rowe *et al.* (1995) and Rowe and Hinchberger (1998). Figure 30 shows the horizontal and vertical displacements of the embankment toe before and after the breakage of reinforcement at 10% strain. After the end of construction, and before the breakage of reinforcement, the velocity of the toe movement diminished with time. However, at the onset of breakage of reinforcement, the toe movement accelerated rapidly (i.e. velocities became very large), and the analysis indicated that the embankment had collapsed upon the failure of the reinforcement at 10% strain.

The results shown in Figures 29 and 30 suggest that the undrained shear strength profile of the foundation soil that would be deduced at a strain rate of 4.8% per hour (i.e. in the range of strain rates recommended by Bishop and Henkel 1962 for triaxial compression tests) might exceed that which could be mobilized in the field. This implies that an arbitrary choice of the strain rate for use in the determination of undrained shear strength for rate-sensitive soils may lead to potential post-construction failure. The conventional undrained analysis method usually makes an assumption that the embankment stability is critical at the end of construction. This assumption could lead to significant errors for rate-sensitive soils, as shown in Figures 29 and 30, and the embankment may fail some time after the end of construction owing to the viscous behaviour of the rate-sensitive soil.

The 'critical stage' of an embankment on a rate-sensitive foundation soil, as defined by Li and Rowe (2001c), can be illustrated in terms of the calculated effective stress path and strain rate at the mid point of the slip surface, as shown in Figure 31. During the initial elastic loading there was some limited pore pressure dissipation and the stress path was nearly vertical while the strain rate increased slightly. After the soil became viscoplastic, the stress path moved towards the failure envelope in an undrained manner and the strain rate increased rapidly. Subsequently the stress path moved above the long-term strength envelope owing to rate effects, and the strain rate reached its maximum at the end of construction. After the end of construction the stress path moved downwards during creep and stress-relaxation, and the mobilized strength of soil decreased with time. The critical stage was reached when the stress path moved to the lowest location corresponding to the lowest undrained shear strength. At this point the embankment was least stable, and the corresponding point in time is called the 'critical stage'. After the critical stage, the stress-relaxation was overcome by the increase in effective stresses due to significant consolidation, and the stress path eventually moved away from the failure envelope. The strain rate decreased rapidly with time during consolidation.

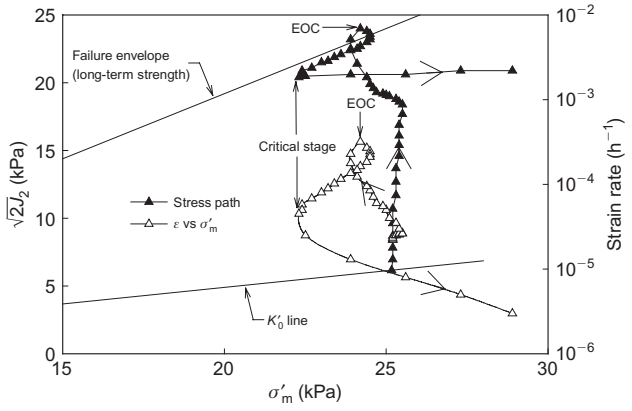

Figure 31. Stress path and strain rate at Point A for 5 m-high reinforced ($J = 2000$ kN/m) embankment over Soil C-R1 (CR = 10 m/month; J_2 = second stress invariant)

The strain rate corresponding to the critical stage is defined as the 'critical strain rate'. At the critical stage, the mobilized shear strength is the operational shear strength that governs the stability of the embankment. Li and Rowe (2002) have shown that the operational undrained shear strength of foundation soil beneath an embankment is the strength that will be mobilized when the soil is sheared at the critical strain rate.

8.2. Operational shear strength of rate-sensitive soils

The importance of strain rate effects on embankment stability problems is discussed by Bjerrum (1973), Tavenas and Leroueil (1980) and Leroueil and Marques (1996). For design, the undrained shear strength may be estimated using field tests, such as the vane test (Bjerrum 1972) and laboratory tests (Ladd and Foott 1974). Field vane tests usually involve high strain rates and hence may be expected to overestimate the undrained shear strength of soils. It has been shown that the undrained shear strength based on field vane tests may significantly overestimate the operational undrained strength of rate-sensitive soils (Rowe and Hinchberger 1998; Rowe and Li 2002). The strain rate for triaxial undrained compression tests is typically recommended to be between 2.4 and 4.8%/h (Bishop and Henkel 1962) or 0.5 and 1.0%/h (Germaine and Ladd 1988). These rates may be much faster than the critical strain rate of soil under an embankment (Li 2000). A design based on the measured strength without appropriate correction may lead to post-construction failure of embankments (Rowe and Li 2002). It is convenient to introduce a correction factor, μ, to the measured shear strength to allow for strain-rate effects (i.e. $s_{ou} = \mu\, s_u$). However, the correction factor for strain-rate effect has been difficult to choose owing to the uncertainty about the strain rate that governs the operational shear strength in foundation soils.

Based on the critical stage concept, Li and Rowe (2002) have proposed an undrained shear strength correction factor that can be calculated using critical strain rate. It has been shown that the embankment reaches the critical stage some time after construction during the period of significant creep and stress-relaxation before significant consolidation occurs. A power function is used to correlate the undrained shear strength at different strain rates as follows:

$$\frac{s_{ou}}{s_u} = \left(\frac{\dot{\varepsilon}_c}{\dot{\varepsilon}}\right)^{1/m} \tag{26}$$

where m = the strain-rate parameter (similar to the viscoplastic model parameter n); $\dot{\varepsilon}_c$ = the critical strain rate; $\dot{\varepsilon}$ = the strain rate used in tests; and $s_{ou:}$ = the field operational undrained strength.

The parameter m in Equation 26 represents the gradient of the undrained shear strength and logarithmic strain-rate relationship. Based on a summary of a number of clays reported in the literature, Hinchberger (1996) has shown that the parameter m ranges from approximately 42 for remolded Boston Blue clay to 11 for highly sensitive Mastemyr clay. Soga and Mitchell (1996) have shown that m typically ranges between 15 and 29 for a number of clays. Li (2000) has calculated critical strain rates that are in the range of 5×10^{-6}/h and 5×10^{-5}/h with a typical value of 1×10^{-5}/h for a relatively wide range of rate-sensitive foundation soils. As a first approximation it appears that, for a typical rate-sensitive soil, the average critical strain rate of 1×10^{-5}/h may be used to estimate the operational undrained shear strength. From Equation 26 the correction factor, μ, that is applied to the measured shear strength, obtained at a known strain rate $\dot{\varepsilon}$, can be expressed as follows:

$$\mu = \left(\frac{1 \times 10^{-5}/\text{h}}{\dot{\varepsilon}}\right)^{1/m} \tag{27}$$

Equation 27 is usually expected to be conservative since partial drainage during construction can significantly reduce the creep deformations of foundation soils and improve the stability, as shown by Rowe and Li (2002).

8.3. Creep effect of foundation soils on reinforcement strains

The deformations and excess pore pressures may increase after the end of construction owing to undrained creep of a rate-sensitive foundation soil. The deterioration in embankment stability after the end of construction and before the critical stage can result in mobilization of reinforcing force and strains necessary to maintain stability. In the Sackville reinforced embankment case, the recorded reinforcement strain increased significantly with time at constant fill thickness after the foundation soil became viscoplastic (Figures 5 and 6 and Rowe and Hinchberger 1998).

Li (2000) has shown that for reinforced embankments over rate-sensitive soils the time-dependent reinforcement strain is significant until the critical stage is reached. For example, Figure 32 shows the development of maximum reinforcement strain from the beginning of construction to 95% consolidation for a 5 m-high reinforced (J = 2000 kN/m) embankment constructed over foundation Soil C-R1 at rates of CR = 2 and 10 m/month. It can be seen that the maximum reinforcement strains are relatively small at the end of construction and increase significantly between the end of construction (EOC) and the critical stage. For the CR = 10 m/month case, the maximum reinforcement strains at the end of construction, the critical stage and 95% consolidation are 1.4%, 4.6% and 5.5% respectively. The increase of reinforcement strain during the significant creep period between the end of construction and the critical stage is over three times. After the critical stage, the reinforcement strain only increases slightly during consolidation.

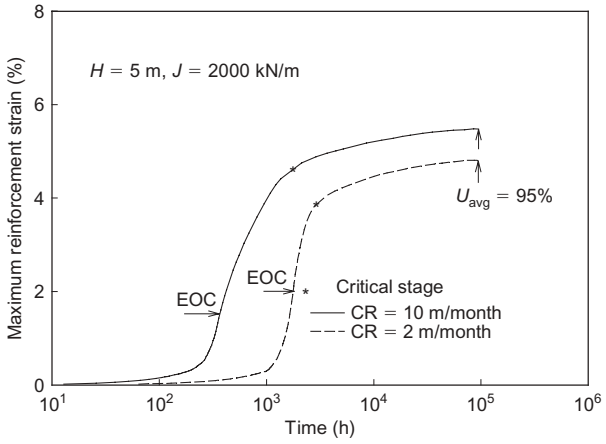

Figure 32. Short-term and long-term reinforcement strains developed for embankments over Soil C-R1

The maximum reinforcement strains developed both during and after the construction were found to be affected by the partial drainage conditions, as shown in Figure 32. One could also presume that for a strain-rate-dependent foundation soil the faster the construction rate the more stable the embankment in the short term. However, for this case, a five-fold decrease in construction rate results in a reduction of reinforcement strains from 4.5% to 3.7% at the critical stage, and from 5.5% to 4.8% at 95% consolidation. Thus it is evident that the partial consolidation of the foundation soil during construction reduces the post-construction creep deformations of the foundation soils and the strain in the reinforcement.

9. CREEP OF REINFORCEMENT IN EMBANKMENTS

9.1. Background

Experimental studies have shown that geosynthetic materials, especially those made from polyethylene (PE) and polypropylene (PP), are all susceptible to creep (e.g. McGown *et al.* 1984; Christopher *et al.* 1986; Greenwood and Myles 1986; Leshchinsky *et al.* 1997). Generally, the creep rate of polyethylene (PE) is greater than that of polypropylene (PP), which is greater than that of polyester (PET) (den Hoedt 1986; Jewell and Greenwood 1988; Greenwood 1990). The stress–strain behaviour of a geosynthetic is also a function of strain rates (Shrestha and Bell 1982; Rowe and Ho 1986; Bathurst and Cai 1994; Nothdurft and Janardhanam 1994; Boyle *et al.* 1996) and ambient temperature (Wrigley 1987; Jewell and Greenwood 1988; Bush 1990; Koerner *et al.* 1993; Rimoldi and Montanelli 1993; Thornton *et al.* 1998).

The time-dependent behaviour of a reinforced embankment may result from the time-dependent response of both the geosynthetic reinforcement and the soft cohesive foundation soils (Li and Rowe 2001d). The viscoelastic

nature of geosynthetics can significantly influence the performance of reinforced embankments over soft soils.

9.2. Viscous behaviour of geosynthetics during construction and after construction

The construction of embankments over soft foundations usually takes some days or months owing to construction conditions associated with poor foundations. The construction time can influence the response of geosynthetic reinforcement to the embankment loading owing to the viscous behaviour of the geosynthetic (Li and Rowe 2001b). Figure 33 shows the calculated net embankment height against fill thickness for two embankments constructed over foundation Soil B (Figure 15). The first embankment is reinforced using a uniaxial HDPE geogrid reinforcement (G2) with wide-width tensile stiffness $J_{5\%} = 1940$ kN/m at 5% strain, ultimate strength $T_{ult} = 166$ kN/m, and a creep strain of 5% over a 20-month period at 40% of the ultimate strength. The second embankment is reinforced using an elastic reinforcement with a stiffness $J = 1940$ kN/m, which is equal to the secant stiffness at 5% strain of the geogrid reinforcement measured from the wide-width tensile test at a strain rate of 10%/min. Both embankments are constructed at a construction rate of 10 m/month. For the first embankment, the failure height H_f (i.e. the fill thickness at failure) is 4.88 m and the mobilized reinforcement strain at embankment failure was 5.3%. At this strain, the mobilized reinforcement tensile force at embankment failure is 67 kN/m. It is evident that the mobilized force for embankment construction is significantly less than the ultimate strength, $T_{ult} = 166$ kN/m. This implies that in the design of a reinforced embankment the ultimate strength of the reinforcement should not be directly used to estimate the factor of safety.

For the embankment reinforced using a perfectly elastic reinforcement, the embankment failure height H_f is 5.7 m and the failure strain was 9.4%. The mobilized tension in reinforcement was 182 kN/m. It is evident that the viscous behaviour of the geogrid reinforcement can affect the embankment failure height, and the maximum mobilized reinforcement tensile strain and force. It follows from Figure 33 that the creep-sensitive reinforcement behaves in a less stiff manner than it would in a tensile test at a relatively fast strain rate (i.e. 10% /min) owing to creep and stress-relaxation of reinforcement during construction. Consequently, the viscoelastic behaviour of geosynthetic reinforcement decreases the embankment stability (Figure 33) in terms of the embankment failure height. For the case shown in Figure 33 the viscous behaviour of the reinforcement during embankment construction decreases the embankment failure height by 14%.

For creep-sensitive geosynthetic reinforcement, the reinforcement strain may significantly increase with time owing to creep of the reinforcement after embankment construction (Li and Rowe 2001b). Figure 34 shows (solid lines) the development of reinforcement strain with time up to 98% consolidation for embankments reinforced using HDPE (upper figure) and PET (lower figure) geosynthetics. Also shown (dashed lines) are the strains that would be developed if the reinforcement was inviscid with stiffness selected such that, at the end of construction, the reinforcement strain is the same as that developed in the viscous reinforcement. Thus, the difference between the solid and dashed lines represents the creep strain due to the viscous nature of the reinforcement. For the PET reinforcement, creep is insignificant and the long-term reinforcement strains for both viscous and inviscid reinforcement are practically the same. For the HDPE geogrid reinforcement, there is about 2% creep strain between the end of construction and the time of 98% consolidation.

9.3. Mobilized and isochronous reinforcement stiffness

Based on the reinforcement force and strain developed, the mobilized reinforcement stiffness (i.e. secant stiffness) can be calculated at different times. For the HDPE geogrid reinforced embankment shown in Figure 33, the reinforcement stiffness developed at embankment failure is 1264 kN/m, which is only 65% of the tensile stiffness at 5% strain determined by an ASTM D 4595 test (ASTM, 2001). This implies that for creep-sensitive reinforcement the tensile stiffness from the standard test can significantly

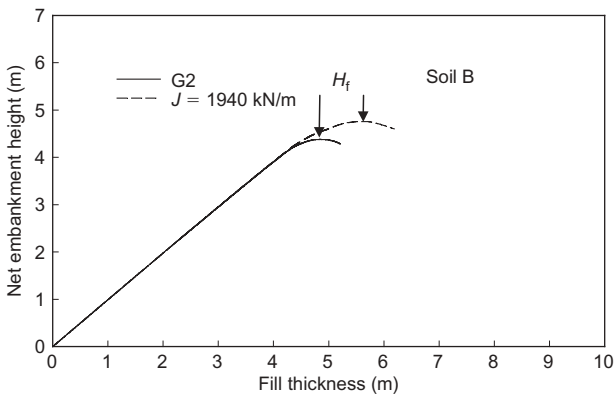

Figure 33. Variation of net embankment height with fill thickness

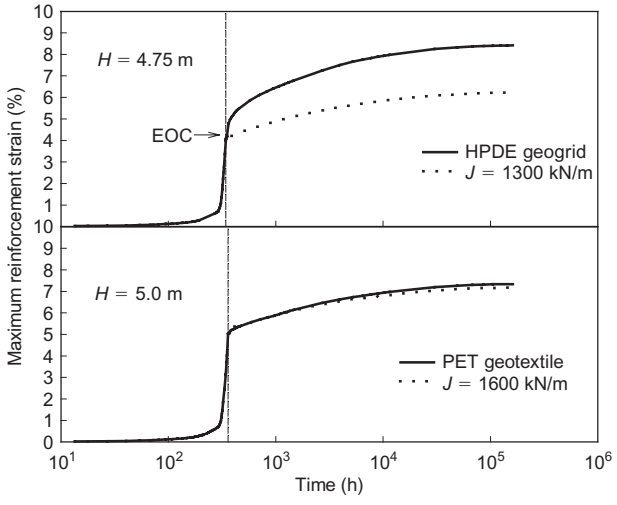

Figure 34. Variation of reinforcement strain with time for embankments over Soil profile B

overestimate the reinforcement stiffness that can be developed in the field.

Li and Rowe (2001b) showed that the mobilized reinforcement stiffness is time-dependent stiffness, and isochronous stiffness can reasonably and conservatively represent the operational stiffness at the end of construction. It is recommended that the isochronous stiffness should be used in design to estimate the mobilized reinforcing force at the end of embankment construction. Figure 35 compares the mobilized reinforcement stiffness with isochronous stiffness deduced from in-isolation creep test data during and after the construction of the HDPE geogrid and PET geosynthetic-reinforced embankments. It can be seen that the mobilized stiffness decreases with time and very closely approaches the isochronous stiffness in the long term. The time dependence of the mobilized reinforcement stiffness is affected by the creep sensitivity of the geosynthetics. The mobilized stiffness at the end of construction is 60% and 95% of the secant stiffness at 5% strain measured in the standard test at a tensile strain rate of 10%/min for HDPE and PET reinforcement respectively. This indicates that the force in the reinforcement at the end of embankment construction may be significantly lower than expected in design owing to the viscous behaviour of geosynthetic reinforcement during embankment construction. This highlights the need for care when applying tensile stiffness from standard load–strain tests (e.g. D 4595; ASTM 2001) to deduce the design tensile force. In addition to creep effects, consideration should be given to potential construction damage of reinforcement (Allen and Bathurst 1994, 1996).

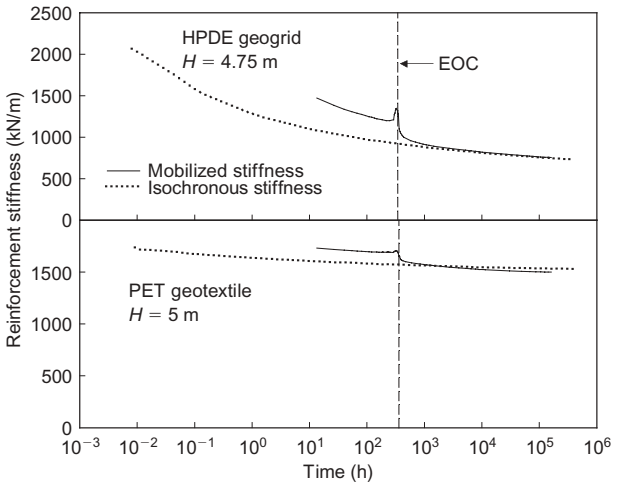

Figure 35. Variation of reinforcement tensile stiffness with time

9.4. Effect of reinforcement creep on deformations

Creep and stress-relaxation of geosynthetic reinforcement can potentially allow an increase in foundation deformation that could be excessive in some cases. Li and Rowe (2001b) have shown that creep of the basal embankment reinforcement during the post-construction period can result in embankment slope movements along the potential slip surface.

Figure 36 shows the contours of maximum shear strain in the foundation Soil B that corresponds to a 2.4% increase in reinforcement tensile strain between the end of construction and 98% consolidation for a particular case. Here, the creep strain of the reinforcement at a constant embankment fill thickness during the time between the end of construction and 98% consolidation was 2%. It is evident that reinforcement creep and stress-relaxation allow an increase in the shear deformations of the foundation soil. The maximum increase of foundation shear strain is over 8%, which is more than four times the creep strain of the reinforcement. This suggests the need for care

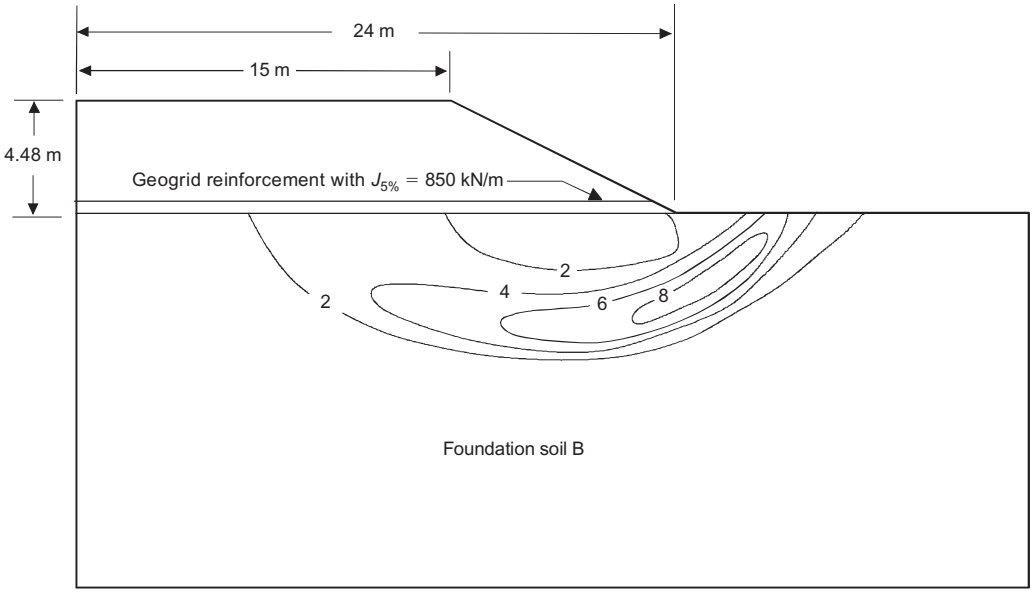

Figure 36. Contours of maximum shear strain (%) in foundation Soil B for 4.5 m-high reinforced embankment due to increase in reinforcement strain of 2.4% between end of construction and 98% consolidation

when using creep-sensitive reinforcement for embankments on soft foundations.

10. CONCLUSIONS

The current state of the art with respect to the behaviour and design of geosynthetic-reinforced embankments over soft foundations has been examined. The conclusions that can be drawn from this study are summarized below.

- Field case histories have shown that the use of geosynthetic reinforcement provides a cost-effective alternative to conventional construction methods.
- The use of PVDs increases the embankment stability owing to the significant strength gain associated with consolidation during construction.
- The maximum reinforcement strains observed in the field under working conditions are usually lower than the design values. This can be attributed to a combination of the low shear strength adopted in design, partial consolidation of foundation soils during construction, and working stress conditions.
- The finite element method provides an effective tool to analyze reinforced embankments constructed over soft deposits. However, careful consideration must be given to the type of constitutive relationships which are used to model the components of the reinforced embankment system.
- Geosynthetic reinforcement can substantially increase embankment failure heights for embankments constructed over both rate-sensitive and rate-insensitive soft cohesive soils.
- The reinforcement has the greatest beneficial effect for embankments on deposits where the soil strength increases with depth.
- In general, for a soft cohesive soil without PVDs, limit equilibrium approaches assuming undrained conditions can provide reasonable agreement with the observed performance.
- The increase in stability due to the use of stiff reinforcement is greater under partially drained conditions than under undrained conditions.
- The beneficial effect of partial consolidation during embankment construction is enhanced by the use of reinforcement.
- The use of reinforcement can reduce the number of construction stages and consequently shorten the construction time.
- Prefabricated vertical drains may allow significant partial consolidation of the foundation soil during embankment construction. In this case, the assumption of undrained conditions is too conservative, and the strength gain of the foundation soil due to partial consolidation can be considered in design using the method proposed by Li and Rowe (2001a).
- The combination of reinforcement and PVDs efficiently increases embankment stability and reduces deformations. The design procedure proposed by Li and Rowe (2001a) integrates consideration of reinforcement and PVDs in design.
- Embankments can be safely constructed over peat soils using reinforcement in combination with appropriate construction rates. The major effect of reinforcement is to reduce lateral spreading and increase stability.
- For reinforced embankments constructed over rate-sensitive foundation soils, the viscoplastic behaviour of foundation soils can significantly reduce embankment stability after the end of construction. With respect to stability, the critical stage occurs at the end of essentially undrained creep and stress-relaxation of foundation soils before significant consolidation occurs.
- The critical strain rate at which foundation soils will deform at the critical stage controls the operational strength of foundation soils at the time that failure is most likely.
- Based on available information, it appears that the operational undrained shear strength of rate-sensitive foundation soils can be estimated by applying the correction factor proposed by Li and Rowe (2002). More field verification of this approach is desirable.
- The use of reinforcement can significantly reduce the creep deformations of the foundation soils: the stiffer the reinforcement, the less creep deformation is developed.
- The strain-rate characteristics of viscoplastic foundation soils may result in a small reinforcement strain being mobilized at the end of construction. However, owing to creep of the foundation soils after construction, reinforcement strains may increase significantly with time before the critical stage is reached.
- During embankment construction, viscoelastic geosynthetic reinforcement behaves less stiffly than implied by wide-width tensile tests at a standard rate of 10%/min owing to strain-rate effects.
- The isochronous stiffness measured from in-isolation creep tests appears to reasonably and conservatively represent the end of construction stiffness of the reinforcement.
- The creep and stress-relaxation of reinforcement can magnify the foundation shear deformations.
- Consolidation, the viscous characteristics of rate-sensitive clays, and the viscous nature of geosynthetics all contribute to the time-dependent behaviour of reinforced embankments.

The use of geosynthetic reinforcement to increase the stability of embankments on conventional soft clay and peat foundations is now well established and discussed herein. This paper has highlighted some of the recent advances in:

(1) considering the effect of partial consolidation during construction and in particular combining the effect of reinforcement and PVDs;
(2) understanding the behaviour of reinforced embankment on rate-sensitive soils and allowing for their rate-sensitive nature in design; and

(3) understanding the effect of reinforcement creep on embankment performance.

11. ACKNOWLEDGEMENTS

The work reported in this paper was funded by the Natural Sciences and Engineering Research Council of Canada. The authors very gratefully acknowledge the careful review of the paper by R. J. Bathurst.

NOTATIONS

SI units are given in parentheses.

b footing width (m)
B embankment crest width (m)
B_{max} pore pressure parameter (dimensionless)
c' effective cohesion intercept of Mohr–Coulomb failure envelope (Pa)
C_c compression index (dimensionless)
C_r recompression index (dimensionless)
C_k hydraulic conductivity change index (dimensionless)
$C_{O/C}$ coefficient of consolidation in overconsolidated stress range (dimensionless)
$C_{N/C}$ coefficient of consolidation in normally consolidated stress range (dimensionless)
CR construction rate (m/s)
D depth or thickness of a soil deposit (m)
D_e effective diameter of drain influence zone (m)
d depth of failure zone (m)
d_s diameter of smear zone (m)
d_w equivalent diameter of drain (m)
E_u undrained elastic modulus (Pa)
e_o initial void ratio (dimensionless)
f_c partial factor for cohesion strength (dimensionless)
f_ϕ partial factor for friction strength (dimensionless)
f_γ partial factor for unit weight (dimensionless)
H embankment height (m)
H_c height of an unreinforced embankment at collapse (m)
H_d length of longest drainage path in vertical direction (m)
H_f embankment failure (m)
h embankment height (m)
h^* thickness (m)
I_q stress influence factor (dimensionless)
J reinforcement stiffness (N/m)
$J_{5\%}$ secant reinforcement stiffness at 5% strain (N/m)
J_{req} required reinforcement stiffness (N/m)
L length of single drain (m)
K_A coefficient of active earth pressure (dimensionless)
K_0' coefficient of lateral earth pressure at rest (dimensionless)
k_h hydraulic conductivity of undisturbed soil in horizontal direction (m/s)
k_s hydraulic conductivity of disturbed soil in smear zone (m/s)
k_v hydraulic conductivity of soil in vertical direction (m/s)
m strain-rate parameter (dimensionless)
N_c bearing capacity factor (dimensionless)
n cotangent of embankment slope (dimensionless)
nr number of regions (dimensionless)
q_s uniform surcharge (Pa)
q_u ultimate bearing capacity (Pa)
R radius of slip circle (m)
S spacing of PVDs (m)
s_{ou} field operational undrained strength (Pa)
s_u undrained shear strength (Pa)
s_{uo} undrained shear strength at ground surface (Pa)
Δs_{uc} increase in shear strength of soil along embankment centreline (Pa)
Δs_{uf} increase in shear strength of soil along failure surface (Pa)
T reinforcement force (N/m)
T_1 thrust force in fill and clay-fill interface shear (N/m)
T_2 pullout capacity of reinforcement (N/m)
T_3 allowable reinforcement force governed by strength (N/m)
T_4 allowable reinforcement force governed by allowable strain (N/m)
T_{ult} ultimate reinforcement strength (N/m)
T_{req} required reinforcement tensile force (N/m)
t time (s)
t_C construction time (s)
$t_{O/C}$ time for soil in overconsolidated stress range during consolidation (s)
$\overline{U}$ average degree of consolidation (dimensionless)
$\overline{U}_f$ average degree of consolidation of soil on a slip surface (dimensionless)
$\overline{U}_{N/C}$ average degree of consolidation in normally consolidated stress range (dimensionless)
$\overline{U}_{O/C}$ average degree of consolidation in overconsolidated stress range (dimensionless)
u excess pore pressure (Pa)
Δu excess pore pressure (Pa)
W_i weight due to embankment fill of region i (N)
x footing surcharge width (m)
x_c x coordinate of centre of slip circle (m)
x_i centroid x coordinate of region i (m)
Z_R distance of slip circle to ground surface (m)
z depth (m)
z_c z coordinate of circle centre (m)
α strength ratio (dimensionless)
β strength ratio (dimensionless)
δ clay–fill interface adhesion factor (dimensionless)
γ unit weight (N/m^3)
γ_f bulk unit weight of the embankment fill (N/m^3)

γ_{fill}	bulk unit weight of the embankment fill (N/m^3)
ε_a	allowable reinforcement strain (dimensionless)
$\dot{\varepsilon}$	strain rate used in tests (s^{-1})
$\dot{\varepsilon}_c$	critical strain rate (s^{-1})
θ	angle (degrees)
μ	undrained shear strength correction factor (dimensionless)
ρ_c	gradient of undrained shear strength with depth (Pa/m)
σ_m'	effective mean stress (Pa)
σ_{mi}'	initial effective mean stress (Pa)
σ'_p	preconsolidation stress (Pa)
σ_N	normal stress acting on the reinforcement (Pa)
σ_v'	vertical effective stress (Pa)
σ_{vo}'	initial vertical effective stress (Pa)
$\Delta\sigma_m$	applied mean stress along potential failure surface (Pa)
$\Delta\sigma_x$	applied stress in x-axis direction (Pa)
$\Delta\sigma_y$	applied stress in y-axis direction (Pa)
$\Delta\sigma_z$	applied stress in z-axis direction (Pa)
$\Delta\sigma(t)$	applied embankment stress at time t (Pa)
$\Delta\sigma_v$	change in vertical stress (Pa)
ϕ	friction angle of embankment fill (degree)
Ω	nondimensional parameter (dimensionless)

ABBREVIATIONS

ASTM	American Society for Testing and Materials
ERAT	equilibrium ratio
EOC	end of construction
GG	geogrid
GT	geotextile
HDPE	high-density polyethylene
MOFILL	overturning moment of fill
MOPT	overturning moment due to horizontal thrust pressure
MRR	restoring moment of reinforcement
MRSOIL	restoring moment of soil
NRR	no reinforcement required
NW	nonwoven
PE	polyethylene
PET	polyester
PF	potential failure
PVD	prefabricated vertical drain
REAP	reinforced embankment analysis program
W	woven

REFERENCES

Adams, J. I. (1961). Laboratory compression tests on peat. *Proceedings 7th Muskeg Research Conference*, NRC Technical Memorandum 41, 36–54.

Allen, T. M. & Bathurst, R. J. (1994). Characterization of geosynthetic load–strain behavior after installation damage. *Geosynthetics International*, **1**, No. 2, 181–199.

Allen, T. M. & Bathurst, R. J. (1996). Combined allowable strength reduction factor for geosynthetic creep and installation damage. *Geosynthetics International*, **3**, No. 3, 407–439.

Andrawes, K. Z., McGown, A., Mashhour, M. M. & Wilson-Fahmy, R. F. (1980). Tension Resistance inclusions in soils. *Journal of Geotechnical Engineering Division, ASCE*, **106**, No. GT12, 1313–1326.

ASTM (2001) *Standard Test Method for Tensile Properties of Geotextiles by the Wide-Width Strip Method*, D 4595. West Conshohocken, PA: American Society for Testing and Materials.

Bassett, R. H. & Yeo, K. C. (1988). The behaviour of a reinforced trial embankment on soft shallow foundations. *International Geotechnical Symposium on Theory and Practice of Earth Reinforcement*, Fukuoka, pp. 371–376.

Bathurst, R. J. & Cai, Z. (1994). In-isolation cyclic load-extension behaviour of two geogrids. *Geosynthetics International*, **1**, No. 1, 1–19.

Bathurst, R. J., Karpurapu, R. G. & Jarrett, P. M. (1992). Finite element analysis of a geogrid reinforced soil wall. In *Grouting, Soil Improvement and Geosynthetics* (eds Borden, R. H., Holtz, R. O. and Juran, I.), Vol. 2, pp. 1213–1224. ASCE Geotechnical Special Publication No. 30.

Bergado, D. T., Long, P. V., Loke, K. H., Christopher, B. R. & Delmas, P. (1994). Geotextile reinforcement in full scale test embankment on soft ground. *Proceedings of the 5th International Conference on Geotextiles, Geomembranes and Related Products, Singapore*, **1**, 21–24.

Biot, M. A. (1941). General theory of three-dimensional consolidation. *Journal of Applied Physics*, **12**, 155–164.

Bishop, A. W. & Henkel, D. J. (1962). *The Measurement of Soil Properties in the Triaxial Test*, 2nd end. London: Edward Arnold.

Bjerrum, L. (1972). Embankments on soft ground. *Proceedings, ASCE Specialty Conference on Earth and Earth-Supported Structures, Purdue University, West Lafayette*, Vol. 2, pp. 1–54.

Bjerrum, L. (1973). Problems of soil mechanics and construction on soft clays. *Proceedings of the 8th International Conference on Soil Mechanics and Foundation Engineering, Moscow*, **3**, 111–159.

Borges, J. L. & Cardoso, A. S. (1998). Influence of geometry and construction sequence on reinforced embankments on soft soils. *Proceedings of the 6th International Conference on Geosynthetics*, Atlanta, USA, **2**, 789–792.

Boutrop, E. & Holtz, R. D. (1983). Analysis of embankments on soft ground reinforced with geotextiles. *Proceedings of 8th European Conference on Soil Mechanics and Foundation Engineering, Helsinki*, **2**, 469–472.

Boyle, S. R., Gallagher, M. & Holtz, R. D. (1996). Influence of strain rate, specimen length and confinement on measured geotextile properties. *Geosynthetics International*, **3**, No. 2, 205–225.

Bush, D. I. (1990). Variation of long term design strength of geosynthetics in temperature up to 40°C. *Proceedings of the 4th International Conference on Geotextiles and Geomembranes and Related Products, The Hague*, **2**, 673–676.

Carrillo, N. (1942) Simple two- and three-dimensional cases in theory of consolidation of soils. *Journal of Mathematics and Physics*, **21**, No. 1, 1–5.

Casagrande, A. & Wilson, S. D. (1951). Effect of rate of loading on the strength of clays and shales at constant water content. *Géotechnique*, **2**, 251–263.

Chai, J. C. & Bergado, D. T. (1993a). Some techniques for finite element analysis of embankments on soft ground. *Canadian Geotechnical Journal*, **30**, 710–719.

Chai, J. & Bergado D. T. (1993b). Performance of reinforced embankment on Muar clay deposit. *Soils and Foundations*, **33**, No. 4, 1–17.

Christopher, B. R., Holtz, R. D. & Bell, W. D. (1986). New tests for determining the in-soil stress–strain properties of geotextiles. *Proceedings of the 3rd International Conference on Geotextiles, Vienna*, **3**, 683–688.

Clough, R. W. & Woodward, R. J. (1967). Analysis of embankment stresses and deformations. *Journal of Soil Mechanics and Foundation Division, ASCE*, **93**, No. 4, 529–549.

Crooks, J. H. A., Becker, D. E., Jeffries, M. G. & McKenzie, K. (1984). Yield behaviour and consolidation. I: Pore pressure response. *Proceedings ASCE Symposium on Sedimentation Consolidation Models, Prediction and Validation*, San Francisco, pp. 356–381.

Davis, E. H. & Booker, J. R. (1973). The effect of increasing strength with depth on the bearing capacity of clays. *Géotechnique*, **23**, No. 4, 551–563.

den Hoedt, G. (1986). Creep and relaxation of geotextile fabrics. *Geotextiles and Geomembranes*, **4**, 83–92.

Duarte, F. M. & Satterlee, G. S. (1989). Case study of a geotextile reinforced levee on a soft clay foundation. *Proceedings Geosynthetics '89 Conference, San Diego*, 160–171.

Duncan, J. M. & Schaefer, V. R. (1988). Finite element consolidation analysis of embankments. *Computers and Geotechnics*, **6**, No. 2, 77–93.

Duncan, J. M., Schaefer, V. R., Franks, L. W. & Collins, S. A. (1987). Design and performance of a reinforced embankment for Mohicanville Dike No. 2 in Ohio. *Transportation Research Record*, **1153**, 15–25.

Edil, T. B. & Dhowian, A. W. (1981). At-rest lateral pressure of peat soils. *Journal of Geotechnical Engineering Division, ASCE*, **107**, No. GT2, 201–217.

Flaate, K. & Rygg, N. (1964). Sawdust as embankment fill on peat bogs. *Proceedings 9th Muskeg Research Conference*, NRC, ACSSM Technical Memorandum 81, 136–149.

Fowler, J. & Edris, E.V. Jr (1987). Fabric reinforced embankment test section, Plaquemine Parish, Louisiana, USA. *Geotextiles and Geomembranes*, **6**, 1–51.

Fowler, J. & Koerner, R. M. (1987). Stabilization of very soft soils using geosynthetics. *Proceedings Geosynthetics '87 Conference, New Orleans*, **1**, 289–299.

Fritzinger, S. A. (1990). Subaqueous use of high-strength geotextiles. *Proceedings 4th International Conference on Geotextiles and Geomembranes and Related Products, The Hague*, **1**, 143–148.

Germaine, J. T. & Ladd, C. C. (1988). Triaxial testing of saturated cohesive soils. In Advanced *Triaxial Testing of Soil and Rock*, ASTM Special Technical Publication No. 977, pp. 421–459. Philadelphia, PA: ASTM.

Graham, J., Crooks, J. H. A. & Bell, A. L. (1983). Time effects on the stress–strain behaviour of natural soft clays. *Géotechnique*, **33**, 727–340.

Greenwood, J. H. (1990). The creep of geotextiles. *Proceedings 4th International Conference on Geotextiles and Geomembranes and Related Products, The Hague*, **2**, 645–650.

Greenwood, J. H. & Myles, B. (1986). Creep and stress relaxation of geotextiles. *Proceedings 3rd International Conference on Geotextiles, Vienna*, **3**, 821–824.

Hadj-Hamou, T. & Bakeer, R. (1991). *Comparative Study of a Geogrid and a Geotextile Reinforced Embankment*. ASCE, Geotechnical Special Publication No. 27, pp. 923–934.

Haliburton, T. A. (1981). Use of engineering fabric in road and construction. *Proceedings of a Seminar on the Use of Synthetic Fabrics in Civil Engineering, Toronto*, pp. 66–94.

Hansbo, S., Jamiolkowski, M. & Kok, L. (1981). Consolidation by vertical drains. *Géotechnique*, **31**, No. 1, 45–66.

Hashizume, H., Konami, T., Kawahara, H., Nagao, K. & Imayoshi, H. (2000). The effect of high strength geosynthetic to stabilize an embankment on soft ground. *Proceedings of 2nd European Geosynthetics Conference, Bologna*, **1**, 245–249.

Hinchberger, S. D. (1996). *The Behaviour of Reinforced and Unreinforced Embankments on Rate Sensitive Clayey Foundations*. PhD thesis, Faculty of Graduate Studies, University of Western Ontario, Canada.

Hinchberger, S. D. & Rowe, R. K. (2003). Geosynthetic reinforced embankments on soft clay foundations: predicting reinforcement strain at failure. *Geotextiles and Geomembranes*, **21**, No. 3, 151–175.

Hird, C. C. & Kwok, C. M. (1989). Finite element studies of interface behaviour in reinforced embankments on soft ground. *Computers and Geotechnics*, **8**, No. 2, 111–131.

Hird, C. C. & Kwok, C. M. (1990). Parametric studies of the behaviour of a reinforced embankment. *Proceedings 4th International Conference on Geotextiles, Geomembranes and Related Products, The Hague*, **1**, 137–142.

Hird, C. C., Pyrah, I. C. & Russell, D. (1992). Finite element modelling of vertical drains beneath embankments on soft ground. *Géotechnique*, **42**, No. 3, 499–511.

Hird, C. C., Pyrah, I. C., Russell, D. & Cinicioglu, F. (1995). Modelling the effect of vertical drains in two-dimensional finite element analyses of embankments on soft ground. *Canadian Geotechnical Journal*, **32**, No. 5, 795–807.

Hird, C. C., Russell, M. D. & Jewell, R. A. (1996). The stability of single-stage constructed reinforced embankments on soft clay. *Proceedings of Institution of Civil Engineers: Geotechnical Engineering*, **125**, 191–205.

Holtz, R. D. (1987). Preloading with prefabricated vertical strip drains. *Geotextiles and Geomembranes*, **6**, 109–131.

Holtz, R. D., Jamiolkowski, M. B., Lancellotta, R. & Pedroni, R. (1991). *Prefabricated vertical drains: design and performance*. CIRIA Ground Engineering Report: Ground Improvement. Oxford: Butterworth-Heinemann, 131 pp.

Holtz, R. D., Christopher, B. R. & Berg, R. R. (1997). *Geosynthetic Engineering*. Richmond, BC, Canada: BiTech Publishers.

Holtz, R. D., Shang, J. Q. & Bergado, D. T. (2001). Soil improvement. In *Geotechnical and Geoenvironmental Engineering Handbook* (ed. R. K. Rowe), pp. 429–462. Norwell, MA: Kluwer Academic.

Humphrey, D. N. & Holtz, R. D. (1987). Reinforced embankments: a review of case histories. *Geotextiles and Geomembranes*, **6**, No. 4, 129–144.

Humphrey, D. N. & Holtz, R. D. (1989). Effect of surface crust on reinforced embankment. *Proceedings Geosynthetics '89, San Diego*, 136–147.

Industrial Fabrics Association International (2004). Specifier's guide. *Geotechnical Fabrics Report*, **21**, No. 9.

Ingold, T. S. (1982). An analytical study of geotextiles reinforced embankments. *Proceedings 2nd International Conference on Geotextiles, Las Vegas*, **3**, 683–688.

Jamiolkowski, M., Lancellotta, R. & Wolski, W. (1983). Precompression and speeding up consolidation: general report. *Proceedings 8th European Conference on Soil Mechanics, Helsinki*, **3**, 1201–1226.

Jewell, R. A. (1982). A limit equilibrium design method for reinforced embankments on soft foundations. *Proceedings 2nd International Conference on Geotextiles, Las Vegas*, **4**, 671–676.

Jewell, R. A. (1988). The mechanics of reinforced embankments on soft soils. *Geotextiles and Geomembranes*, **7**, 237–273.

Jewell, R. A. (1996). *Soil Reinforcement with Geotextiles*, Construction Industry Research and Information Association Special Publication 123. London: Thomas Telford.

Jewell, R. A. & Greenwood, J. H. (1988). Long term strength and safety in steep soil slopes reinforced by polymer materials. *Geotextiles and Geomembranes*, **7**, 81–118.

Kabbaj, M., Tavenas, F. & Leroueil, S. (1988). In situ and laboratory stress–strain relationships. *Géotechnique*, **38**, No. 1, 83–100.

Keenan, G. H., Landva, A. O., Valsangkar, A. J. & Comier, R. S. (1986). Performance and failure of test embankment on organic silty clay. *Proceedings of the Conference on Building on Marginal and Derelict Land*, Glasgow, Vol. 2, pp. 417–428.

Kerr, J. R., Bennett, B., Perzia, O. N. & Perzia, P.A. (2001). Geosynthetic reinforced highway embankment over peat. *Proceedings Geosynthetics '2001, Portland, OR*, 539–552.

Kjellman, W. (1948). Accelerating consolidation of fine-grained soils by means of cardboard wicks. *Proceedings of 2nd International Conference on Soil Mechanics and Foundation Engineering, Rotterdam*, 302–305.

Koerner, R. M. (1997). *Designing With Geosynthetics*, 4th edn. Prentice Hall, Upper Saddle River, New Jersey, USA.

Koerner, R. M., Hsuan, Y. & Lord, A.E. (1993). Remaining technical barriers to obtaining general acceptance of geosynthetics. *Geotextiles and Geomembranes*, **12**, No. 1, 1–52.

Kulhawy, F. H. & Mayne, P. W. (1990). *Manual on Estimation Soil Properties for Foundation Design*. Palo Alto, CA: Electric Power Research Institute.

Ladd, C. C. (1991). Stability evaluation during staged construction. *Journal of Geotechnical Engineering*, **117**, No. 4, 540–615.

Ladd, C. C. & Foott, R. (1974). New design procedure for stability of

soft clays. *Journal of the Geotechnical Engineering Division, ASCE*, **100**, No. GT7, 763–786.

Landva, A. O. (1980). Vane testing in peat. *Canadian Geotechnical Journal*, **17**, No. 1, 1–19.

Landva, A. O., Korpijaakko, E. O. & Pheeney, P. E. (1983). Geotechnical classification of peats and organic soils. *ASTM Special Technical Publication 820,* pp. 37–51.

Lau, K. W. K. & Cowland, J. W. (2000). Geosynthetically enhanced embankments for the Shenzhen River. *Advances in Transportation and Geoenvironmental Systems Using Geosynthetics*, Geotechnical Special Publication No. 103, ASCE, Virginia, pp. 140–161.

Lea, N. D. & Brawner, C. O. (1963). Highway design and construction over peat deposits in the lower mainland of British Columbia. *Highway Research Board Research Record*, **7**, 1–33.

Leroueil, S. & Marques, M. E. S. (1996). Importance of strain rate and temperature effects in geotechnical engineering. *Proceedings 1996 ASCE National Convention*, Washington DC, Geotechnical Special Publication No. 61, pp. 1–60.

Leroueil, S. & Rowe, R. K. (2001). Embankments over soft soil and peat. In *Geotechnical and Geoenvironmental Engineering Handbook* (ed. R. K. Rowe). Norwell, MA: Kluwer Academic, pp. 463–500.

Leroueil, S., Tavenas, F., Mieussens, C. & Peignaud, M. (1978). Construction pore pressures in clay foundations under embankments. Part II: generalized behaviour. *Canadian Geotechnical Journal*, **15**, No. 1, 65–82.

Leshchinsky, D. (1987). Short-term stability of reinforced embankment over clayey foundations. *Soils and Foundations*, **27**, No. 3, 43–57.

Leshchinsky, D., Dechasakulsom, M., Kaliakin, V. N. & Ling, H. I. (1997). Creep and stress relaxation of geogrids. *Geosynthetics International*, **4**, No. 5, 463–479.

Li, A. L. (2000). *Time Dependent Behaviour of Reinforced Embankments on Soft Foundations*. PhD thesis, The University of Western Ontario, London, Canada, 398 pp.

Li, A. L. & Rowe, R. K. (1999a). Reinforced embankments and the effect of consolidation on soft cohesive soil deposits. *Proceedings Geosynthetics '99, Boston*, **1**, 477–490

Li, A. L. & Rowe, R. K. (1999b). Reinforced embankments constructed on foundations with prefabricated vertical drains. *Proceedings 52nd Canadian Geotechnical Conference, Regina*, 411–418.

Li, A. L. & Rowe, R. K. (2001a). Combined effects of reinforcement and prefabricated vertical drains on embankment performance. *Canadian Geotechnical Journal*, **38**, No. 6, 1266–1282.

Li, A. L. & Rowe, R. K. (2001b). Influence of creep and stress-relaxation of geosynthetic reinforcement on embankment behaviour. *Geosynthetics International*, **8**, No. 3, 233–270.

Li, A. L. & Rowe, R. K. (2001c). Effects of viscous behaviour of soft foundation soils on reinforced embankments. *Proceedings 54th Canadian Geotechnical Society Conference, Calgary*, **3**, 1210–1217.

Li, A. L. & Rowe, R. K. (2001d). The time dependent behaviour of reinforced embankments constructed over soft cohesive foundations. *Proceedings of 15th International Conference on Soil Mechanics and Geotechnical Engineering*, Istanbul, **2**, 1651–1656.

Li, A. L. & Rowe, R. K. (2002). Some design considerations for embankments on rate sensitive soils. *ASCE Journal of Geotechnical and Geoenvironmental Engineering*, **128**, No. 11, 885–897.

Litwinowicz, A., Wijeyakulasuriya, C. V. & Brandon, A. N. (1994). Performance of a reinforced embankment on a sensitive soft clay foundation. *Proceedings 5th International Conference on Geotextiles, Geomembranes and Related Products, Singapore*, **1**, 11–16.

Lockett, L. & Mattox, R. M. (1987). Difficult soil problems on Cochrane Bridge finessed with geosynthetics. *Proceedings Geosynthetic '87 Conference, New Orleans*, **1**, 309–319.

Loke, K. H., Ganeshan, V., Werner, G. & Bergado, T. D. (1994). Composite behaviour of geotextile reinforced embankment on soft clay. *Proceedings 5th International Conference on Geotextiles, Geomembranes and Related Products, Singapore*, **1**, 25–28.

Low, B. K., Wong, K. S., Lim, C. & Broms, B. B. (1990). Slip circle analysis of reinforced embankments on soft ground. *Geotextiles and Geomembranes*, **9**, No. 1, 165–181.

Lupien, C., Lefebvre, G., Rosenberg, P., Paré, J. J. & Lavallé, J. G. (1983). The use of fabrics for improving the placement of till on peat foundation. Paper presented at 62nd Annual Meeting of Transportation Research Board, Washington, 17–21 January. Available in *Transport Research Record*, 1983, 54–59.

Matar, M. & Salencon, J. (1977). Capacité portante à une semelle filante sur sol purement cohérent d'épaisseur limitée et de cohésion variable avec la profondeur. *Annales de l'Institut Technique du Bâtiment et des Travaux Publics*, **352**, *Serie: Sols et Fondations*, **143**: 95–107.

Matichard, Y., Tanays, E. & Carton, M. (1994). Geotextile reinforced embankment to cross a peat-bog. *Proceedings 5th International Conference on Geotextiles, Geomembranes and Related Products*, Singapore **1**, 37–40.

Mattox, R. M. & Fugua, D. A. (1995). Use of geosynthetics to construct the Vera Cruz access ramp of the bridge of the Americas, Panama. *Proceedings Geosynthetics '95, Nashville, Tennessee*, **1**, 67–77.

McGown, A., Andrawes, K. Z., Yeo, K. C. & DuBois, D. (1984). The load–strain-time behaviour of tensar geogrids. *Proceedings Symposium on Polymer Grid Reinforcement in Civil Engineering*, SERC/Netlon, London, pp. 11–17.

Milligan, V. & La Rochelle, P. (1984). Design methods for embankments over week soils. *Proceedings Symposium on Polymer Grid Reinforcement in Civil Engineering*, Institution of Civil Engineers, London, pp. 95–102.

Monnet, J., Gourc, J. P. & Mommessin, M. (1986). Study of soil geotextile interaction: a reinforced embankment. *Proceedings 2nd International Symposium on Numerical Models in Geomechanics, Ghent*, 539–542.

Mylleville, B. L. J. & Rowe, R. K. (1988). *Simplified Undrained Stability Analysis for Use in the Design of Steel Reinforced Embankments on Soft Foundations*, GEOT-3–88. Faculty of Engineering Science, University of Western Ontario, 73 pp.

Mylleville, B. L. J. & Rowe, R. K. (1991). On the design of reinforced embankments on soft brittle clays. *Proceedings Geosynthetics '91 Conference, Atlanta, GA*, **1**, 395–408.

Nicholson, D. P. & Jardine, R. J. (1981). Performance of vertical drains at Queenborough bypass. *Géotechnique*, **31**, No. 1, 67–90.

Nothdurft, D. B. & Janardhanam, R. (1994). Influence of polymer viscoelasticity in reinforced soil structure design. *Proceedings 5th International Conference on Geotextiles, Geomembranes and Related Products, Singapore*, 247–250.

Oikawa, H., Sasaki, S. & Fujii, N. (1996). A case history of the construction of a reinforced high embankment. *Proceedings of the International Symposium on Earth Reinforcement, Fukuoka/Kyushu*, pp. 261–266.

Olson, R. E. (1977). Consolidation under time dependent loading. *Journal of the Geotechnical Engineering Division, ASCE*, **103**, No. GT1, 55–60.

Poulos, H. G. & Davis, E. H. (1974). *Elastic Solutions for Soil and Rock Mechanics*. New York: Wiley.

Prandtl, L. C. (1920). Uber die harte plastischen korper. *Nachrichten von der Gesellschaft der Wissenschaften zu Goettingen, Mathematisch-Physikaliasche Klasse*, 74–85.

Raymond, G. P. (1969). Construction method and stability of embankments on muskeg. *Canadian Geotechnical Journal*, **6**, 81–96.

Rimoldi, P. & Montanelli, F. (1993). Creep and accelerated creep testing for geogrids. *Proceedings Geosynthetics '93, Vancouver*, **3**, 773–787.

Ripley, C. F. & Leonoff, C. E. (1961). Embankment settlement behaviour on deep peat. *Proceedings 7th Muskeg Research Conference*, NRC Technical Memorandum No. 71, 185–204.

Rowe, R. K. (1982). The analysis of an embankment constructed on a geotextile. *Proceedings 2nd International Conference on Geotextiles, Las Vegas*, vol. 3, 677–682.

Rowe, R. K. (1984). Reinforced embankments: analysis and design. *Journal of Geotechnical Engineering, ASCE*, **110**, No. GT2, 231–246.

Rowe, R. K. (1997). Reinforced embankment behaviour: lessons from a number of case histories. *Proceedings of the Symposium on Recent Developments in Soil and Pavement Mechanics*, Rio de Janeiro, pp. 147–160.

Rowe, R. K. & Hinchberger, S. D. (1998). The significance of rate effects in modelling the Sackville test embankment. *Canadian Geotechnical Journal*, **35**, No. 3, 500–516.

Rowe, R. K. & Ho, S. K. (1986). Determination of geotextile stress–strain characteristics using a wide strip test. *Proceedings 3rd International Conference on Geotextiles, Vienna*, **3**, 885–890.

Rowe, R. K. & Li, A. L. (1999). Reinforced embankments over soft foundations under undrained and partially drained conditions. *Geotextiles and Geomembranes*, **17**, No. 3, 129–146.

Rowe, R. K. & Li, A. L. (2001). Insights from case histories: reinforced embankments and retaining walls. *Proceedings International Symposium on Earth Reinforcement, Kyushu*, pp. 31–60.

Rowe, R. K. & Li, A. L. (2002). Behaviour of reinforced embankments on soft rate sensitive soils. *Géotechnique*, **52**, No. 1, 29–40.

Rowe, R. K. & Mylleville, B. L. J. (1989). Consideration of strain in the design of reinforced embankments. *Proceedings Geosynthetics '89, San Diego*, 124–135.

Rowe, R. K. & Mylleville, B. L. J. (1990). Implications of adopting an allowable geosynthetic strain in estimating stability, *Proceedings 4th International Conference on Geotextiles, Geomembranes and Related Products, The Hague*, **1**, 131–136.

Rowe, R. K. & Mylleville, B. L. J. (1996). A geogrid reinforced embankment on peat over organic silt: a case history. *Canadian Geotechnical Journal*, **33**, No. 1, 106–122.

Rowe, R. K. & Soderman, K. L. (1984). Comparison of predicted and observed behaviour of two test embankments. *Geotextiles and Geomembranes*, **1**, No. 2, 143–160.

Rowe, R. K. & Soderman, K. L. (1985a). An approximate method for estimating the stability of geotextile reinforced embankments. *Canadian Geotechnical Journal*, **22**, No. 3, 392–398.

Rowe, R. K. & Soderman, K. L. (1985b). Geotextile reinforcement of embankments on peat. *Geotextiles and Geomembranes*, **2**, No. 4, 277–298.

Rowe, R. K. & Soderman, K. L. (1986). Reinforced embankments on very poor foundations. *Geotextiles and Geomembranes*, **4**, 65–81.

Rowe, R. K. & Soderman, K. L. (1987a). Stabilization of very soft soils using high strength geosynthetics: the role of finite element analyses. *Geotextiles and Geomembranes*, **6**, No. 1–3, 53–80.

Rowe, R. K. & Soderman, K. L. (1987b). Reinforcement of embankments on soils whose strength increases with depth. *Proceedings Geosynthetics '87, New Orleans*, 266–277.

Rowe, R. K., MacLean, M. D. & Barsvary, A. K. (1984a). The observed behaviour of a geotextile reinforced embankment constructed on peat. *Canadian Geotechnical Journal*, **21**, No. 2, 289–304.

Rowe, R. K., MacLean, M. D. & Soderman, K. L. (1984b). Analysis of a geotextile reinforced embankment constructed on peat. *Canadian Geotechnical Journal*, **21**, No. 3, 563–576.

Rowe, R. K., Gnanendran, C. T., Landva, A. O. & Valsangkar, A. J. (1995). Construction and performance of a full-scale geotextile reinforced test embankment, Sackville, New Brunswick. *Canadian Geotechnical Journal*, **32**, No. 3, 512–534.

Rowe, R. K., Gnanendran, C. T., Landva, A. O. & Valsangkar, A. J. (1996). Calculated and observed behaviour of a reinforced embankment over soft compressible soil. *Canadian Geotechnical Journal*, **33**, No. 2, 324–338.

Rowe, R. K., Gnanendran, C. T., Valsangkar, A. J. & Landva, A. O. (2001). Performance of a test embankment constructed on an organic clayey silt deposit. *Canadian Geotechnical Journal*, **38**, No. 6, 1283–1296.

Schaefer, V. R. & Duncan, J. M. (1988). Finite element analyses of the St Alban test embankments. Geotechnical Special Publication, No. 18, ASCE, pp. 158–177.

Schimelfenyg, P., Fowler, J. & Leshchinsky, D. (1990). Fabric reinforced containment dike, New Bedford superfund site. *Proceedings 4th International Conference on Geotextiles and Geomembranes and Related Products, The Hague*, **1**, 149–154.

Sharma, J. S. & Bolton, M. (2001). Centrifugal and numerical modeling of reinforced embankments on soft clay installed with wick drains. *Geotextiles and Geomembranes*, **19**, 23–44.

Shimel, S. & Gertje, H. (1997). The use of geotextiles for roadway embankments over soft soils. *Proceedings Geosynthetics '97*, Long Beach, 25–38.

Shrestha, S. C. & Bell, J. R. (1982). Creep behavior of geotextiles under sustained loads. *Proceedings 2nd International Conference on Geotextiles, Las Vegas*, Vol. III, 769–774.

Soga, K. & Mitchell, J. K. (1996). Rate-dependent deformation of structured natural clays. *Proceedings 1996 ASCE National Convention*, Washington DC, Geotechnical Special Publication No. 61, pp. 243–257.

Tavenas, F. & Leroueil, S. (1980). The behaviour of embankments on clay foundations. *Canadian Geotechnical Journal*, **17**, No. 2, 236–260.

Taylor, D. W. (1948). *Fundamentals of Soil Mechanics*. New York: John Wiley & Sons.

Thornton, J. S., Paulson, J. N. & Sandri, D. (1998). Conventional and stepped isothermal methods for characterizing long term creep strength of polyester geogrids. *Proceedings 6th International Conference on Geosynthetics, Atlanta*, **2**, 691–698.

Varadarajan, A., Sharma, K. G. & Aly, M. A. A. (1997). Finite element analyses of reinforced embankment foundation. *International Journal for Numerical and Analytical Methods in Geomechanics*, **23**, No. 2, 103–114.

Varuso, R. J., Grieshaber, J. B. & Nataraj, M. S. (1999). Design and analysis of a geosynthetic levee test section. *Proceedings Geosynthetics '99, Boston*, 451–464.

Volk, J. C., Hunt, R. E., Leshchinsky, D., Diloreto, R. & Collins, T. G. (1994). Reinforced embankment over very soft soil: Grassy Sound highway embankment. *Proceedings 5th International Conference on Geotextiles, Geomembranes and Related Products*, Singapore, **1**, 41–48.

Weber, W. G. Jr (1969). Performance of embankments constructed over peat. *Journal of the Soil Mechanics and Foundations Division, ASCE*, **95**, No. SM1, 53–76.

Wrigley, N. E. (1987). Durability and long-term performance of Tensar polymer grids for soil reinforcement. *Material Science Technology*, **3**, 161–170.

The Editors welcome discussion in all papers published in Geosynthetics International. Please email your contribution to discussion@geosynthetics-international.com by 15 August 2005.